2014•2015
FACULTEIT GENEESKUNDE EN LEVENSWETENSCHAPPEN
master in de biomedische wetenschappen

Masterproef

Establishing a moderate contusion spinal cord injury mouse model and testing the therapeutic potential of interleukin-13

Promotor :
Prof. dr. Sven HENDRIX

Copromotor :
dr. Evi LEMMENS

Ellen Donders
Scriptie ingediend tot het behalen van de graad van master in de biomedische wetenschappen

De transnationale Universiteit Limburg is een uniek samenwerkingsverband van twee universiteiten in twee landen: de Universiteit Hasselt en Maastricht University.

universiteit hasselt
KNOWLEDGE IN ACTION

Universiteit Hasselt | Campus Hasselt | Martelarenlaan 42 | BE-3500 Hasselt
Universiteit Hasselt | Campus Diepenbeek | Agoralaan Gebouw D | BE-3590 Diepenbeek

universiteit hasselt | Maastricht University

2014•2015
FACULTEIT GENEESKUNDE EN LEVENSWETENSCHAPPEN
master in de biomedische wetenschappen

Masterproef

Establishing a moderate contusion spinal cord injury mouse model and testing the therapeutic potential of interleukin-13

Promotor :
Prof. dr. Sven HENDRIX

Copromotor :
dr. Evi LEMMENS

Ellen Donders

Scriptie ingediend tot het behalen van de graad van master in de biomedische wetenschappen

universiteit hasselt | Maastricht University

Table of contents

Table of contents ..... **I**

Acknowledgements ..... **III**

List of abbreviations ..... **V**

Summary ..... **VII**

Samenvatting ..... **IX**

1. Introduction **1**

1.1 Human spinal cord injury 1

1.1.1 Etiology 1

1.1.2 Secondary disabilities 1

1.1.3 Spinal cord pathology 2

1.2 Rodent models for spinal cord injury 4

1.3 Pro- and anti-inflammatory cytokines after spinal cord injury 5

1.4 Interleukin-13 5

1.4.1. Interleukin-13 in the central nervous system 6

1.5 Experimental approach 7

2. Materials and methods **9**

2.1 Animals 9

2.2 Surgery 9

2.3 Contusion parameter groups 9

2.4 Interleukin-13 treatment 10

2.5 Locomotion tests 10

2.5.1 Basso mouse scale 10

2.5.2 Rotarod 10

2.6 Histological analysis of spinal cord tissue 11

2.6.1 Perfusion of the animals 11

2.6.2 Immuno-histochemical analysis of spinal cord tissue 11

2.6.3 Histochemical analysis of spinal cord tissue: Oil red O staining 12

2.7 Statistical analysis 12

3. Results **13**

3.1 Murine spinal cord contusion by a 1.5 mm tip creates a too severe injury 13

3.1.1 Contusion injuries induced by a 1.5 mm tip lead to poor functional recovery 13

3.1.2 Lesion size and demyelinated area correlate with functional recovery 13

3.1.3 No significant difference in astrogliosis between the different injury groups 15

3.1.4 Analysis of immune cell infiltration only reveals significant difference in microglia/macrophage infiltration between different injury groups. 17

3.2 Murine spinal cord contusion by a 1 mm tip and a 0.3 mm impact depth creates a moderate injury 19

3.2.1 Contusion injuries caused by a 1 mm tip and a 0.3 mm impact depth result in a moderate spontaneous functional recovery 19

3.2.2 Lesion size and demyelinated area are significantly higher after 0.3 mm impact depth compared to 0.1 mm injuries 20

3.2.3 Astrogliosis is not significantly different between contusions with 0.1 mm and 0.3 mm injury depth 21

3.2.4 Increased microglia/macrophage and foamy macrophage activity in the 0.3 mm injury depth group 21

3.3 IL-13 improves functional recovery after contusion SCI 24

4. Discussion 25

5. Conclusion 29

References 31

Supplemental information 35

Acknowledgements

During the last eight months, I performed my senior practical training at the Biomedical research institute of Hasselt University. The practical training and this thesis would not have been possible without the help of several people. Therefore, I would like to thank everyone who has supported me during my internship.

First, I would like to thank my promotor, Prof. Dr. Sven Hendrix for giving me the opportunity to perform my internship in his research group. His expertise and critical view helped me in becoming a better scientist. Special thanks go to my co-promotor Dr. Evi Lemmens for critically reviewing my thesis. Her daily support and guidance helped me improve my practical work. I would also like to thank her for the nice talks and relaxing moments every once in a while. Furthermore, I would like to thank the other members of the morphology department, team Sven as well as team Ivo, for their help at the lab and for lending me their access cards ☺. I also want to thank my second examiner, Prof. Dr. Bert Brône, for taking the time to look at my project and giving constructive advice.

Of course, the last eight months would not have been the same without my Biomed buddies. Lauren, Cindy, Dorien, Hafida, Len, Yörg, Wim, Jirka and Joris, we have had many stressfull, but also many great moments. Forever I will remember our numerous coffee breaks, crazy Friday afternoon talks, TD's, dinner dates and other fun trips. After all the hard work, we finally made it to fully fledged biomedical scientists!

Next, I want to thank my friends and in particular my fitness buddies. Jolien, Lisa, Alicia, Mitch and Paula, thank you all for making me forget about the stressful moments during our, almost daily, fitness dates! Lastly, special thanks go to my parents, grandparents, my "little" brother and my boyfriend for all their support, not only during this internship, but also during the previous years of my education.

List of abbreviations

SCI	Spinal cord injury
IL	Interleukin
BMS	Basso mouse scale
CNS	Central nervous system
PBS	Phosphate buffered saline
PFA	Paraformaldehyde
GFAP	Glial fibrillary acidic protein
Dapi	4',6-Diamidino-2-phenylindole
MBP	Myelin basic protein
Iba-1	Ionized calcium binding adaptor molecule-1
CD4	Cluster of differentiation 4
M1	Classically activated macrophages
M2	Alternatively activated macrophages
RT	Room temperature
SEM	Standard error of the mean
SD	Standard deviation
Th1	T helper 1
TH2	T helper 2
TGF- β	Transforming growth factor-beta
CCI	Controlled cortical impact
IL-13Ra1	Interleukin-13 receptor subunit alpha-1
IL-13Ra2	Interleukin-13 receptor subunit alpha-2
IL-4R	Interleukin-4 receptor
IL-4Ra	Interleukin-4 receptor subunit alpha
TM	Transmembrane
TNF-α	Tumor necrosis factor alpha
i.p.	Intraperitoneal
ORO	Oil red O
ROI	Region of interest
RGB	Red-green-blue
EAE	Experimental autoimmune encephalomyelitis
T8-T10	Thoracic level 8 to 10

Summary

Introduction: Spinal cord injury (SCI) is a debilitating condition, often resulting in paralysis. The majority of human injuries are contusions resulting from traffic accidents and falls. In SCI, the initial mechanical injury to the spinal cord is followed by an inflammatory reaction. This reaction contributes to neurodegeneration but may also play a role in neuroregeneration. Two days after the initial injury, anti-inflammatory cytokines, such as interleukin-13 (IL-13), are produced by immune cells. Preliminary data of our group suggest a positive effect of IL-13 on functional recovery in a hemisection mouse model for SCI. The goal of this study is to establish a moderate contusion spinal cord injury mouse model and to investigate the therapeutic potential of IL-13 in this clinically relevant SCI model.

Materials and methods: To establish a moderate standardized SCI contusion model, a controlled cortical impact (CCI) stereotactic device was used in which different parameters, such as velocity, dwell time, impact depth and impactor tip width, were manipulated. Differences in tip diameter and impact depth were evaluated with a predetermined velocity and dwell time of 4.6 m/s and 500 ms. Subsequently, the severity of the lesion was determined via analysis of functional recovery, lesion size, demyelinated area and immune cell infiltration. Furthermore, the therapeutic potential of IL-13 was investigated in this contusion SCI model by systemically injecting the cytokine once a day for seven days.

Results: A contusion inflicted by a CCI device with a velocity of 4.6 m/s, a dwell time of 500 ms, a tip diameter of 1 mm and an impact depth of 0.3 mm shows a spontaneous recovery up to occasional plantar stepping after 3 weeks. Furthermore, lesion characteristics as lesion size, demyelinated area, microglia/macrophage activity, foamy macrophage activity and $CD4^+$ T cell infiltration negatively correlate with functional recovery. Moreover, treatment with IL-13 shows a significant increase in functional recovery in this moderate contusion SCI model.

Discussion & conclusions: The contusion caused by a 1 mm tip diameter and a 0.3 mm impact depth creates a moderate SCI. This model can be used to gain mechanistic insights into the basic cellular and molecular biology of the condition. The newly established model shows a small variation, which is essential for a good animal model. Furthermore, the spontaneous functional recovery allows room for improvement with a potential therapy, like IL-13. In the future, this model can be used by our research group to study other therapeutic options for SCI.

Samenvatting

Introductie: Een ruggenmergletsel is een slopende aandoening die vaak resulteert in verlammingsverschijnselen. De meerderheid van de menselijke letsels zijn contusies die veroorzaakt worden door verkeersongevallen. De initiële schade aan het ruggenmerg wordt gevolgd door een ontstekingsreactie. Deze reactie draagt bij aan neurodegeneratie maar kan ook een rol spelen bij neuroregeneratie. Twee dagen na het initiële letsel, worden er anti-inflammatoire cytokines, zoals interleukine-13 (IL-13), geproduceerd door immuun cellen. Preliminaire data van onze onderzoeksgroep suggereren een positief effect van IL-13 op functioneel herstel in een hemisectie muis model voor ruggenmergletsels. Het doel van deze studie is het oprichten van een klinisch relevant contusie muis model voor ruggenmergletsels en het onderzoeken van de therapeutische werking van IL-13 in dit model.

Materiaal en methoden: Een gecontroleerde corticale impactor (CCI) werd gebruikt om het model op te richten. Hierbij kunnen verschillende parameters, zoals snelheid, contactduur, impact diepte en impact tip diameter, aangepast worden om een gestandaardiseerd letsel met een gematigde ernst te bekomen. Verschillen in tip diameter en impact diepte werden getest bij een vaste snelheid en contactduur van 4.6 m/s en 500 ms. De ernst van de lesie werd vervolgens bepaald via de analyse van functioneel herstel, lesie grootte, gedemyeliniseerd gebied en immuun cel infiltratie. Verder werd IL-13 getest als een therapeutische optie in het contusie muis model.

Resultaten: Een contusie veroorzaakt door een CCI met een snelheid van 4.6 m/s, een contactduur van 500 ms, een tip diameter van 1 mm en een impact diepte van 0.3 mm vertoont een spontaan herstel dat leidt tot occasioneel plantair stappen na 3 weken. Lesie karakteristieken zoals lesie grootte, gedemyeliniseerd gebied, microglia/macrofaag activiteit, schuimige macrofaag activiteit en $CD4^+$ T cel infiltratie vertonen een negatieve correlatie met het functioneel herstel. Verder leidt een behandeling met IL-13 tot een significante verbetering in het functioneel herstel in dit contusie model.

Discussie & conclusie: De contusie veroorzaakt door een tip diameter van 1 mm en een impact diepte van 0.3 mm leidt tot een gematigd ruggenmergletsel. Dit muismodel kan gebruikt worden om mechanische inzichten in de cellulaire en moleculaire biologie van de aandoening te verwerven. Het spontane functionele herstel biedt ruimte voor verbetering met een potentiele therapie, zoals IL-13. Verder vertoont het model een kleine variatie, wat een belangrijke eigenschap is voor een goed diermodel. In de toekomst kan dit model ook gebruikt worden om andere mogelijke therapieën voor ruggenmergletsels te testen.

1. Introduction

Spinal cord injury (SCI) is a debilitating condition resulting from a direct or indirect trauma to the spinal cord or its surrounding area. Symptoms of SCI can vary from discomfort to immediate loss of motor and sensory function. The degree of the injury depends on its location along the spinal cord and the severity of the lesion. To date, a fully restorative therapy is not yet available and current therapies focus on relieving the symptoms of this devastating condition. A promising therapy may be the treatment with an anti-inflammatory cytokine, such as interleukin 13 (IL-13).

1.1 Human spinal cord injury

SCI can be anatomically divided into two groups. The most commonly affected region in humans is the cervical spinal cord (43.9% – 61.5%) (1). This type of injury is classified as high SCI whereas lower SCI includes thoracic, lumbar and sacral injuries. The level of injury can be described in two ways. Generally, the first segment that shows neurological loss is defined as the level of injury by neurologists. Contrarily, physiatrists define the injury level as the most caudal segment of the spinal cord that has a normal function (2, 3). Defining the level of injury is important to set a clinical diagnosis, predict future outcomes and determine the appropriate therapy.

1.1.1 Etiology

SCI has an annual incidence of 15 to 50 cases per one million people worldwide (4). Approximately 80% of new cases are males between the age of 15 and 35 years. Most commonly, SCI is caused by traffic accidents. During the last 30 years, SCI caused by traffic accidents increased amongst men under 30 years of age. Furthermore, falls are the second most common etiology, which is mostly observed in the elderly population. Due to the increasing life expectancy in our society, the rising aging population indicates that traumatic SCI resulting from falls is becoming an increasing public health problem (1).

1.1.2 Secondary disabilities

Due to modern care units, the life expectancy of SCI patients is improving. This is accompanied with secondary disabilities in the majority of cases, including impairments in bowel and bladder control, breathing, heart rate, blood pressure and sexual function. Patients can also suffer from trunk instability, spams, chronic pain syndrome and pressure wounds. Furthermore, SCI affects all aspects of the patient's life, including their psychological and socio-economic functioning. For example, social adjustment can be a major issue for the patient and can lead to exclusion from full participation in the society. Frequent hospitalization and lack of autonomy severely affect the quality of life of the injured person. SCI patients often become dependent from their relatives and see themselves as a burden on the family. In most cases, patients are dealing with frustrations, anxiety and a low self-esteem. These psychosocial challenges may result in depressions, sleep disorders and post-traumatic stress.

Furthermore, the majority of patients are not able to keep their job after the injury which results in financial stress. Additionally, the different secondary disabilities are often costly to treat and these increasing health care costs contribute to the financial problems of the injured person. Consequently, SCI has an immense impact on the quality of life of patients and their family (5).

1.1.3 Spinal cord pathology

Human SCI is characterised by an initial trauma, followed by a secondary injury. The initial mechanical injury to the spinal cord mostly results from a fractured vertebra or disk intruding into the spinal cord. This insult results in a compression, contusion, laceration or in rare cases in a complete transection of the spinal cord. Human SCI is most often a contusion which is characterized by fluid-filled cystic cavities. Intact axons can still be present at the injury site but their function is impaired due to demyelination. The loss of oligodendrocytes contributes to this problem (6).

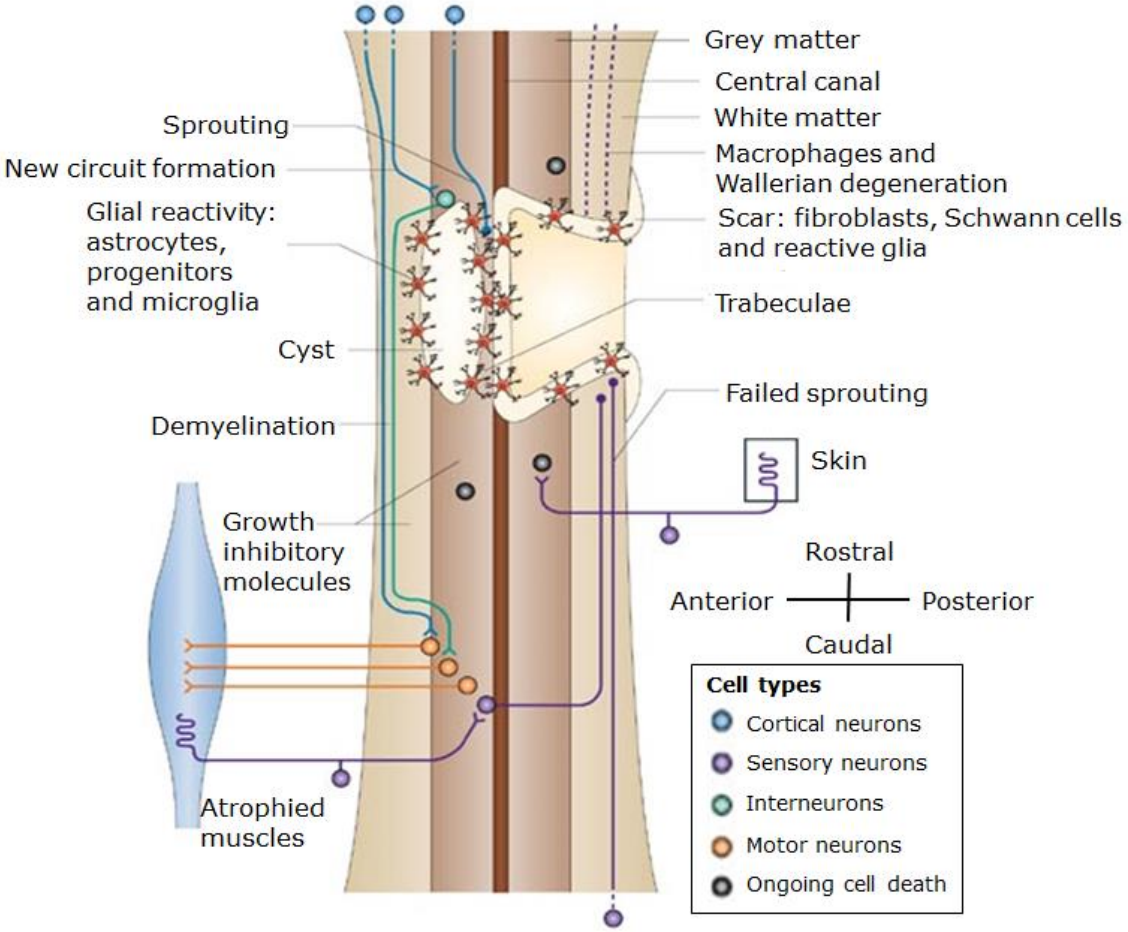

Figure 1: Schematic view of a longitudinal section through an injured spinal cord. After spinal cord injury, many cells die instantly and cystic cavities are formed. Several axons are damaged and fail to regenerate. Some axons, on the other hand, can form new circuits with motor neurons via interneurons, but disconnected axons segments are phagocytosed by macrophages. Peripheral cells invade the injury site, and together with fibroblasts, Schwann cells and reactive glia, form a scar. A certain degree of spontaneous axon remyelination can occur, mainly via Schwann cells from the peripheral nervous system. At areas distal to the central lesion, Wallerian degeneration occurs (figure adapted from (7)).

The SCI pathology can be divided into four phases. First, the initial mechanical insult directly resulting in cell death and ischemia at the site of impact. Second, the spreading of the injury. Next, the immune reactions which are characterized by apoptosis, immune-mediated cell death and axon demyelination (Figure 1). Finally, the stabilization of the lesion by chronic scar formation (8).

Over time, SCI can be divided into three phases, the acute phase (minutes to hours), the sub-acute phase (hours to weeks) and the chronic phase (weeks to months).

Within hours after the initial injury, secondary injury processes start to occur, leading to an augmentation in damage, specifically neuronal and axonal destruction and demyelination in proximity to the lesion site. In addition to necrosis, also apoptotic processes occur at the central lesion. Within a few hours following injury, neutrophils infiltrate the injury site, peaking at 24 hours post-injury. Furthermore, T and B cells are attracted to the injury site. Examples of cytokines involved in the acute phase are IL-1b, IL-6, IL-8, IL-11 and tumor necrosis factor alpha (TNF-α). A portion of these pro-inflammatory factors are produced by type 1 helper T (Th1) cells and contribute in the activation of natural killer cells, neutrophils and M1 macrophages (6, 8, 9). Furthermore, also neurons and glia can produce pro-inflammatory cytokines which contribute to death of neurons and oligodendrocytes (10).

In the sub-acute phase, 48 hours post-injury, neutrophils are largely replaced by microglia, which are the native immune cells of the central nervous system (CNS). Also blood monocytes are recruited to the lesion after 3-7 days. These microglia and monocytes clear the injured area by phagocytosing myelin debris, creating a cystic cavity. Thereupon, this cavity is surrounded by reactive astrocytes developing a glial scar. Astrocytes infiltrate this scar and produce glial fibrillary acidic protein (GFAP). Next to astrocytes, the scar comprises of myelin debris, activated resident microglia and infiltrating blood-borne immune cells, chondroitin sulfate proteoglycans and other growth-inhibitory matrix components (11). Furthermore, the sub-acute phase is characterized by a decrease in pro-inflammatory cytokines and an increase anti-inflammatory cytokines such as transforming growth factor-beta (TGF-β) and IL-10. TGF-β and IL-10 aid in the differentiation of $CD4^+$ T cells towards type 2 helper T (Th2) cells. Thereupon, these T cells produce anti-inflammatory cytokines including IL-4, IL-5 and IL-13. The Th2 cytokines induce the alternatively activated M2 macrophages which also produce anti-inflammatory cytokines (6, 8, 9, 12).

Finally, during the chronic phase, the immune responses are directed towards facilitating the cleaning of the injury site and inducing plasticity. During this phase, a second peak of T cells, macrophages and neutrophils can be observed in the spinal cord. Furthermore, the astrocytic scar stabilizes and depending on the amount of fibroblast infiltration, a dense collagenous scar can be formed. Due to its density and its ability to bind to growth inhibitory molecules, this fibrous scar forms an enormous barrier for regeneration. Additionally, continued apoptosis of oligodendrocytes leads to further axon demyelination causing an extend of myelin debris that also severely inhibits axon growth (6, 9). Although plasticity in initiated, this is insufficient to result in regeneration of the injured spinal cord.

1.2 Rodent models for spinal cord injury

SCI is a multifactorial disorder. Therefore, different animal models are used to study different aspects of this condition. The most widely used models are rodent models. Rodents, like mice and rats, are inexpensive, cheap to house, easy to handle and they can be studied in large numbers. Furthermore, they have a well understood anatomy and there are well defined analyzing techniques available to determine the lesion size, the level of demyelination, the infiltration of immune cells, etc.

A first example of a rodent model for spinal cord injury is the hemisection model. In this model, important motor tracts in the spinal cord, e.g. the corticospinal tract, are transected. A drawback of this model is that this is not a representation of the pathology most commonly observed in humans. On the other hand, this model is well suited for the study of regeneration, degeneration, tissue engineering strategies or plasticity at the axonal level (13).

In contrast to hemisection models, the morphology and pathology of contusion rodent models show more resemblance with the clinical situation. The infiltration of immune cells such as neutrophils, macrophages and lymphocytes at the site of injury contributes to reparative and destructive responses as described previously. These lead to the secondary pathology of SCI resulting in locomotor deficits best represented by contusion models. Contusion injury models can create graded injuries ranging from mild to very severe injuries. Currently, three rodent models for contusion SCI are widely used. One of the first models, the New York University impactor, is based on a weight drop method. More recent models, such as the Ohio State University Electromagnetic SCI Device is based on a displacement-defined device whereas the Precision Systems and Instrumentation Infinite Horizons impactors are based on a force-defined device. These two latter devices can measure the force delivered to the spinal cord at the moment of impact and all three of these devices are known to produce consistent and reproducible injuries. However, it is not known whether force or displacement is important in determining the outcome of the SCI (13, 14).

The contusion injury in this study will be inflicted in mice by the Leica Impact One controlled cortical impact (CCI) stereotactic device. This CCI device can be used to study different injuries, i.e. it can make precisely controlled and positioned impacts on the skull, brain or spinal cord. This aids in studying the anatomical and behavioural effects of neuronal damage. Different parameters, such as velocity, dwell time, impact depth and impactor tip width, can be manipulated with the aim of establishing a standardized lesion with different grades of severity.

An important remark to make is that rats develop large fluid filled cystic cavities similar to the human pathology but are less suitable to study the cellular biology of the injury. Other than rats and humans, mice do not develop these cysts but the lesion gets filled with dense fibrous connective tissue surrounded by glial cells, which is similar to the human situation, but not identical (15). So, depending on the research question, the right animal model must be used.

1.3 Pro- and anti-inflammatory cytokines after spinal cord injury

Inflammation is often described as the most important mechanism of the secondary pathology of SCI, but it also appears to play an essential role in tissue repair. Beneficial, as well as detrimental effects have been ascribed to resident microglia, monocyte-derived macrophages, lymphocytes, antibodies and cytokines. Modulating the immune system towards an anti-inflammatory response is suggested to be a potential therapy to treat spinal cord trauma and other CNS injuries (10).

As briefly mentioned before, exposure to Th1 cytokines leads to the polarization to the M1 subtype. These are the classically activated pro-inflammatory macrophages. During the secondary injury process after SCI, they exhibit neurotoxic and growth inhibitory properties. In this way, they aid in the formation of the glial scar and production of pro-inflammatory mediators. This pro-inflammatory environment can directly cause neural death and contributes to the limited regenerative capacity of the injured area (8). For example, over-expression of IL-6 can lead to enhanced leukocyte infiltration, decreased axonal growth and impaired locomotor recovery (10, 16).

In contrast, exposure to Th2 cytokines leads to the polarization of macrophages to the M2 subtype (17). These alternatively activated M2 macrophages play an important role in counteracting the pro-inflammatory environment produced by the M1 macrophages. In this way, they may contribute to neuroprotection and regeneration of spinal cord tissue and cell renewal. For example, TGF-β1 produced by M2 macrophages after SCI has a positive effect on neurons and decreases oligodendrocyte toxicity (10). Furthermore, M2 macrophages aid in enhancing phagocytosis, scar degradation, angiogenesis and differentiation of neural stem cells as well as helping to restore impaired motor function, clearing reactive oxygen species, etc. (8).

The M1 and M2 macrophages are both present at the center of the lesion during the first days post-injury. After one week, the M2 macrophages disappear and the environment of the injured spinal cord favors the M1 phenotype. In mice, it has been shown that these M1 macrophages remain at the lesion site until one month post-injury. The high M1:M2 ratio is detrimental for CNS repair. A therapeutic approach for SCI may be a switch from M1 to M2 phenotype in the injured spinal cord. The polarization towards a M2 phenotype can promote CNS repair and limit the secondary injury (18). Evidence suggests that therapies to improve recovery after SCI may rely on a reduction of pro-inflammatory molecules and an increase of anti-inflammatory molecules (8). Moreover, studies using vaccination models for CNS injury treatment show that type 2 modulators promote neuronal survival and axon regeneration (6, 9).

1.4 Interleukin-13

IL-13 is an anti-inflammatory cytokine mainly produced by Th2 cells. The effects of IL-13 are mediated via the IL-13 receptors (Figure 2). The type I IL-13 receptor is expressed on many different cells, such as B cells, basophils, eosinophils, mast cells, endothelial cells, fibroblasts, monocytes, macrophages, respiratory epithelial cells, and smooth muscle cells. The type I receptor is a heterodimer of IL-13Ra1 and IL-4Ra. This receptor can also bind IL-4 and is therefore also

known as the type II IL-4 receptor. It is thus not surprising that IL-4 and IL-13 share many functions (19, 20).

Binding of IL-13 to the type I receptor leads to the activation of the JAK-STAT pathway. Thereupon, IRS-1 and IRS-2 become phosphorylated and activated, leading to the induction of several signaling pathways, including the phosphatidylinositol 3 kinase and Ras/mitogen-activated protein kinase pathway (19, 20).

The second IL-13 receptor comprises of IL-13Ra2. Since the expression of IL-13Ra1/ IL-4Ra is sufficient for IL-13 signaling, the IL-13Ra2 receptor is not required for IL-13 function. The *in vitro* expression of IL-13Ra2 leads to an high-affinity binding with IL-13, but is insufficient to generate an intracellular IL-13 response. Moreover, IL-13Ra2 is suspected to be a decoy receptor. It has been shown that IL-13Rα2 also exists in a soluble form and that overexpression of IL-13Rα2 diminishes IL-13 cell signaling (19, 20).

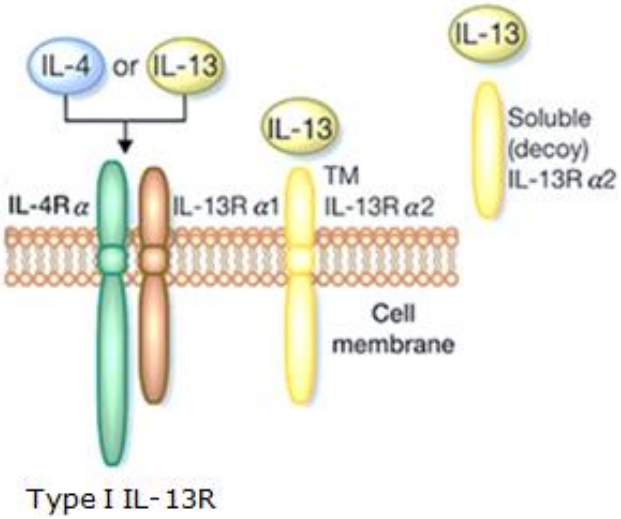

Figure 2: Schematic overview of the IL-13 receptors. Receptors for IL-13 are composed of 3 different subunits: IL-4Rα, IL-13Rα1 and IL-13Rα2. IL-13 can signal through type I IL-13R (IL-13Ra1/IL-4Ra) and can additionally bind to IL-13Ra2. This latter is a decoy receptor and can also occur in soluble form. γc: γ-chain, IL: interleukin, TM: transmembrane (figure adapted from (21)).

1.4.1. Interleukin-13 in the central nervous system

The role of IL-13 in the CNS is not yet completely understood but a beneficial role in neurological disorders is suggested. It is assumed that IL-13 primarily targets macrophages and microglia. As mentioned before, IL-13 is, together with IL-4, involved in the induction of alternatively activated M2 macrophages. Since these macrophages have an anti-inflammatory phenotype, they may be involved in tissue repair and remodeling after a CNS injury (20, 22).

IL-13 also modulates the inflammatory response via the suppression of inflammatory cytokine production, including IL-1b, TNF-α and IL-6 from microglia *in vitro* as well as *in vivo*. In this way, IL-13 can, for example, promote survival in a mouse model for sepsis (23).

Furthermore, IL-13 can also have a protective effect on neurons in CNS disorders. For example, literature describes a neuroprotective role of IL-13 in brains of MS patients (24).

Moreover, it is suggested that IL-13 plays a role in the preservation of injured axons in the spinal cord and the suppression of type 1-mediated autoimmune responses (6, 9). Moreover IL-13 can induce death of microglial cells *in vitro* (25). *In vivo*, death of activated microglia can contribute to improved neural survival (26).

Recently, a beneficial role of this anti-inflammatory cytokine has been suggested by our research team. Nelissen et al. showed decreased IL-13 spinal cord protein levels after hemisection SCI compared to sham operated mice. Furthermore, IL-13 is a substrate for mouse mast cell protease 4 which plays a a protective role in neuroinflammation (27).

Furthermore, preliminary data of our research group indicate an improved functional recovery in a hemisection mouse model for SCI after daily IL-13 administration for 7 sequential days. *In vitro* results show that a low dosis of IL-13 protects against celldeath in spinal cord slices. Moreover, IL-13 improves neurite outgrowth in a dosis-dependent manner in primary neurons and spinal cord slices.

1.5 Experimental approach

Currently, solely the hemisection mouse model is used at our research facility. The primary goal of this study is to establish a moderate contusion injury mouse model for SCI. This model shows a better resemblance to the human pathogenesis.

A moderate contusion model was chosen since a certain degree of spontaneous functional recovery can be observed. If the model is too mild, too much spontaneous recovery is observed and there is no room for improvement with a therapeutic agent. On the other hand, when the animals are too severely injured, the damage in the spinal cord shows more resemblance to the hemisection model. This is not ideal to study therapeutic effects on the secondary pathology of SCI. Conclusively, when choosing a moderate contusion SCI model, animals will have room to functionally improve with a potential therapy.

In order to obtain a moderate contusion, optimization is needed by testing different parameters of the CCI device. Different device-settings will be applied and evaluated via behavioural testing and immuno-histochemical analysis of the spinal cord tissue. According to previous research in a rat contusion injury model, the most reproducible CCI model is obtained by using a velocity of 4.6 m/s, a dwell time of 500 ms, an impact depth of 0.5 mm and an impactor tip width of 2 mm (28). The injury model will now be established in mice since contusions in mice are characterized by a densely packed injury site and are therefore ideal to study mechanistic insights into the basic cellular and molecular biology of SCI. When a moderate spontaneous recovery is observed in the injured animals in accordance to literature findings, the contusion model is established.

Furthermore, the therapeutic potential of IL-13 will be investigated in this model. The effect of IL-13 on functional recovery, lesion volume, demyelinated area, astrogliosis and immune cell infiltration will be explored. This study will lead to a better understanding of the therapeutic mechanisms of IL-13 in a clinically relevant model of spinal cord injury which may contribute to the development of a future therapy.

2. Materials and methods

2.1 Animals

SCI was performed in 10-week-old female Balb/c mice (Harlan, the Netherlands), which were housed in a conventional animal facility at Hasselt University under regular conditions, i.e. on a 12 h light–dark schedule, in a temperature-controlled room (± 20°C) and with water and food ad libitum; all experiments were approved by the local ethical committee of Hasselt University and were performed according to the guidelines on the protection of animals used for scientific purposes described in Directive 2010/63/EU.

2.2 Surgery

Mice were deeply anesthetized by either an intraperitoneal (i.p.) injection of medetomidine (1 mg/kg bodyweight; Domitor, Janssen Animal Health, Orion Pharma, Germany) followed by an i.p. injection of ketamin (75 mg/kg bodyweight; Nimatek, Eurovet, Belgium) after 5 min. Alternatively, isoflurane (Isoflo, Abbott, Belgium) was used. A laminectomy was performed at thoracic level 8 to 10 (T8-T10) (Figure 3A). Next, a contusion injury was performed using the Leica Impact One (Leica Microsystems, Illinois, USA) CCI device. The tip of the impactor was positioned in line with the surface of the dura, retracted and then lowered at the desired depth, with the chosen velocity and dwell time as described in the next section. After the contusion was performed, the dura was punctured to relieve the pressure on the spinal cord caused by bleeding underneath the dura-surface. Next, the muscles were sutured and the back skin was closed with wound clips. Furthermore, mice received subcutaneous injections of the analgesic buprenorphine (1.2 µg/mouse; Temgesic, Val d'Hony Verdifarm, Belgium). Also an i.p. injection of 20% glucose (800 µl/mouse) and atipamezole (0.5 mg/ kg body weight; Antisedan, Elanco, Orion Pharma, Belgium) was given post-surgery. A drop of NaCl (0,9%) was applied on each eye to prevent them from drying out. Furthermore, mice were placed in an incubator for two hours at 33^{o}C to avoid hypothermia. Mice also received antibiotic Baytril (2 ml/l of 10% solution; Bayer, Belgium) in their drinking water, starting 2 days before until 2 weeks after surgery, to prevent them from infections. Furthermore, the health status of the animals was evaluated daily and bladders were manually emptied once a day until reflex voiding function returned.

2.3 Contusion parameter groups

Based on values from the literature to induce a moderate contusion SCI in rats, different parameters, such as velocity, dwell time, impact depth and impactor tip width, were adjusted to the desired settings. The most reproducible CCI model in rats is obtained using a velocity of 4.6 m/s, a dwell time of 500 ms, an impact depth of 0.5 mm and an impactor tip width of 2 mm (28). Similarly, the velocity and dwell time were set at 4.6 m/s and 500 ms, respectively. Furthermore, the optimal impact depth and impactor tip width were determined by testing 3 variations in impact depth, i.e. 0.1 mm, 0.3 mm and 0.5 mm, with an impactor tip width of 1 mm, and 2 variations in impact depth, i.e. 0.1 mm and 0.3 mm, with an impactor tip width of 1.5 mm (Table 1). The 2 mm tip was found to be too wide for the mouse spinal cord.

Table 1: Different parameter groups tested with the CCI device.

Velocity	Dwell time	Impactor tip width	Impact depth
4.6 m/s	500 ms	**1 mm**	**0.1 mm**
4.6 m/s	500 ms	**1 mm**	**0.3 mm**
4.6 m/s	500 ms	**1 mm**	**0.5 mm**
4.6 m/s	500 ms	**1.5 mm**	**0.1 mm**
4.6 m/s	500 ms	**1.5 mm**	**0.3 mm**

CCI: controlled cortical impact. SCI: spinal cord injury.

2.4 Interleukin-13 treatment

After testing the different parameter combinations (Table 1), a moderate contusion was established when using a velocity of 4.6 m/s, a dwell time of 500 ms, an impactor tip width of 1 mm and an impact depth of 0.3 mm. Therefore, these parameters were used to investigate the therapeutic potential of IL-13 in SCI. Female Balb/c mice were randomly assigned to 2 groups, i.e. a IL-13-treated group and a Phosphate buffered saline (PBS) treated control group. The IL-13 treated group received an i.p. injection of murine IL-13 (500 ng; Peprotech, Belgium) in 200 µl PBS immediately after SCI once each day during 7 sequential days. The PBS group, received an i.p. injection of 200 µl PBS immediately after SCI once each day during 7 sequential days.

2.5 Locomotion tests

2.5.1 Basso mouse scale

Starting one day post-surgery, functional recovery was evaluated daily for one week using the Basso mouse scale (BMS) (29). This is a 10-point locomotion rating scale based on hind limb movements made in an open field during a 4 min interval (0 = complete hind limb paralysis; 9 = normal locomotion) (Table S1). Scoring was performed by an investigators blinded to the experimental groups. After this first week of daily measurements, mice were scored every other day. Data obtained by locomotion testing were analyzed only including mice that survived until perfusion. When differences in BMS scores were observed between different hind limbs, the average of both values was taken.

2.5.2 Rotarod

After allowing mice to recover for 7 days, rotarod performance (30) analysis was be performed for 7 sequential days. After a first week of daily measurements, mice were scored every other day. Mice are placed on an accelerated rolling rod for max. 300 s (Ugo Basile, Comeris VA, Italy). The rod accelerates from 2 rotations per minute to 15 per minute. The latency to fall/jump from the rod is automatically recorded since the animals fall onto a trigger plate. Mice were trained in at least two sessions before the injury in order to be able to stay on this rod for as long as physically possible.

2.6 Histological analysis of spinal cord tissue

2.6.1 Perfusion of the animals

Three weeks after injury, mice were transcardially perfused after receiving an overdose of Nembutal (60 mg/kg bodyweight i.p.; CEVA Logistics, Belgium). Perfusion was performed using ringer solution containing heparin, followed by 4% paraformaldehyde. After perfusion, spinal cords were dissected and placed overnight in 5% sucrose in 4% PFA. The next day, spinal cords were transferred to a 30% sucrose solution 1x PBS for one day. Next, spinal cords were embedded in Tissue Tek (O.C.T. Compound, Sakura, Ireland) and frozen in liquid nitrogen-cooled isopentane (GPR Rectapur, VWR, Belgium) at -50°C. Afterwards, longitudinal cryosections (10 µm) were made with a Leica CM 3050s cryostat.

2.6.2 Immuno-histochemical analysis of spinal cord tissue

The spinal cord sections were pre-incubated with 10% goat serum in PBS containing 0.05% Triton X-100 for 30 min at room temperature (RT). Next, primary antibodies were incubated overnight at 4°C (Table 2). Following repeated washing steps with PBS, secondary antibodies were incubated for 1h at RT (Table 2). Furthermore, Dapi (4',6-Diamidino-2-phenylindole) counterstaining was performed for 10 min and sections were mounted with fluorescent mounting medium.

Table 2: Primary and secondary antibodies used for immunohistochemistry.

	GFAP	**MBP**	**Iba-1**	**CD4**
Primary antibody	Mouse anti-mouse GFAP (1/500; Sigma-Aldrich, Belgium)	Rat anti-mouse MBP (1/250; Millipore, Belgium)	Rabbit anti-mouse Iba-1 (1/250; Wako, Germany)	Rat anti-mouse CD4 (1/250; BD Biosciences, Belgium)
Secondary antibody	Goat anti-mouse Alexa Fluor 568 (1/250; Invitrogen, Belgium)	Goat anti-rat Alexa Fluor 488 (1/250; Invitrogen, Belgium)	Goat anti-rabbit Alexa Fluor 488 (1/250; Invitrogen, Belgium)	Goat anti-rat Alexa Fluor 568 (1/250; Invitrogen, Belgium)

GFAP: glial fibrillary acidic protein. MBP: myelin basic protein. Iba-1: ionized calcium-binding adapter molecule 1. CD4: cluster of differentiation 4. 1/250, 1/500: antibody dilutions in 0.05% Triton X-100 and 1% goat serum in 1x phosphate buffered saline.

Immunohistochemistry was analyzed with fluorescence microscopy (Nikon Eclipse 80i, Nikon Instruments, USA), by an investigator blinded to experimental groups. The same exposure-time was applied for all sections of the same experiment. Further image analysis was performed using ImageJ open source software (National Institute of Health, USA). The lesion size and demyelinated area were determined by using anti-GFAP and anti-MBP antibodies respectively and delineating and measuring the GFAP and MBP negative area in ImageJ. The infiltration of $CD4^+$ T cells was analyzed manually by counting the number of cells via double staining with Iba-1 to exclude $CD4^+$ microglial cells. GFAP and Iba-1 expression were quantified via intensity analysis within square areas of 100 µm × 100 µm extending from 600 µm cranial to 600 µm caudal from the lesion border. When analyzing Iba-1 intensity, one additional measurement was performed in the middle of the lesion.

2.6.3 Histochemical analysis of spinal cord tissue: Oil red O staining

Spinal cord sections were stained with Oil red O (ORO) (Sigma, Belgium) to analyze the level of foamy macrophage activity (% of ORO ingested cells). Sections were incubated with 0.5% ORO solution in isopropanol 3/5 diluted with Milli-Q water for 10 min. Furthermore sections were counterstained with heamatoxylin for 5 min and mounted with aqueous mounting solution. Pictures were taken at a 10x magnification for analysis with ImageJ. In the area with the most intense ORO staining, a region of interest (ROI) of 31416 μm^2 was delineated by a circle or an ellipse, depending on the shape of this area. Within the ROI, pixels with an intensity within predetermined red-green-blue (RGB) threshold values were counted as a percentage of the total amount of pixels in this ROI. The threshold values were determined to distinguish background from specific staining and were kept constant for all measurements.

2.7 Statistical analysis

Locomotion tests and intensity analysis were analyzed with Prism 5.0 software (GraphPad Software, USA) using two-way ANOVA for repeated measurements with the Bonferroni post-hoc test. Differences between two groups were evaluated using the nonparametric two-tailed Mann–Whitney U-test. Three groups were compared using the Kruskal-Wallis test. Differences were considered statistically significant when $p < 0.05$.

3. Results

3.1 Murine spinal cord contusion by a 1.5 mm tip creates a too severe injury

3.1.1 Contusion injuries induced by a 1.5 mm tip lead to poor functional recovery

Contusion spinal cord injury was performed in female Balb/c mice via the Impact One CCI device with a predetermined velocity and dwell time of 4.6 m/s and 500 ms, respectively. First, two variations in impact depth, 0.1 mm and 0.3 mm, were tested with a tip diameter of 1.5 mm. Functional recovery was analyzed until 3 weeks post-injury via BMS scoring (Table S1) as described by Basso *et al.* (29). A hallmark of improved functional recovery is the development of plantar stepping. After 3 weeks, still none of the animals were capable of occasional plantar stepping. The majority of animals merely reached a average score of 1.5, meaning that they can only move their ankle joint. Moreover, the BMS score was not significantly different between the two injury groups (Figure 3). Furthermore, during the rotarod performance test, most animals only used their forelimbs to stay on the rod. Therefore, this test did not show a representation for hindlimb motor coordination, balance and strength (data not shown). Conclusively, the 1.5 mm tip diameter creates a too severe contusion SCI in mice.

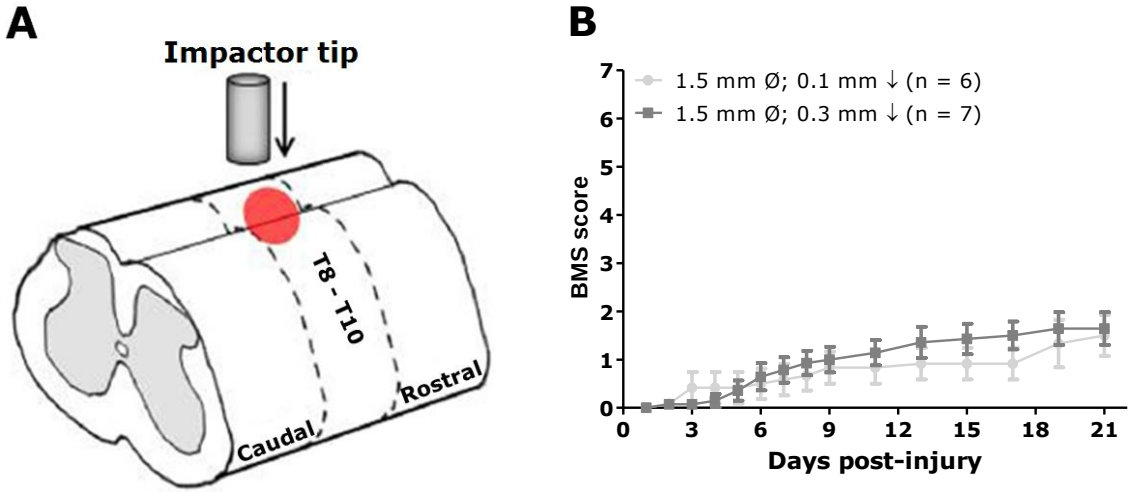

Figure 3: Contusion SCI with a tip diameter of 1.5 mm creates a too severe injury. Mice which received a contusion SCI at T8-T10 (A) with a depth (↓) of 0.1 mm or 0.3 mm and a 1.5 mm tip diameter (Ø) did not show a significant difference in functional recovery (B). After three weeks, the mean BMS score per group did not exceed 3, meaning that the animals are not capable of dorsal stepping or plantar paw placement. Analysis of locomotion tests only included mice perfused after 3 weeks, eliminating animals with a BMS value higher than 3 at day 1. Data represent mean ± SEM. T: thoracic level. BMS: Basso mouse scale. SCI: spinal cord injury. (Figure A adapted from (31))

3.1.2 Lesion size and demyelinated area correlate with functional recovery

Next, it was evaluated whether a different SCI severity affects the lesion size and demyelinated area. GFAP immunohistochemistry was used to evaluate the lesion size, since $GFAP^+$ astrocytes delineate CNS lesions (Figure 4A). Furthermore, MBP was used to investigate the level of demyelination as this is a major component of the myelin sheath (Figure 5A).

Statistical analysis shows no significant difference in lesion size (Figure 4B) and demyelinated area (Figure 5B) between the 0.1 mm and 0.3 mm injuries. Interestingly, when comparing lesion size (Figure 4C) and demyelinated area (Figure 5C) according to locomotor recovery (BMS score), a higher BMS score is associated with a smaller lesion size and demyelinated area and vice-versa. Furthermore, correlation analysis revealed a slightly significant negative correlation between BMS score and lesion size (Figure 4D) and demyelinated area (Figure 5D).

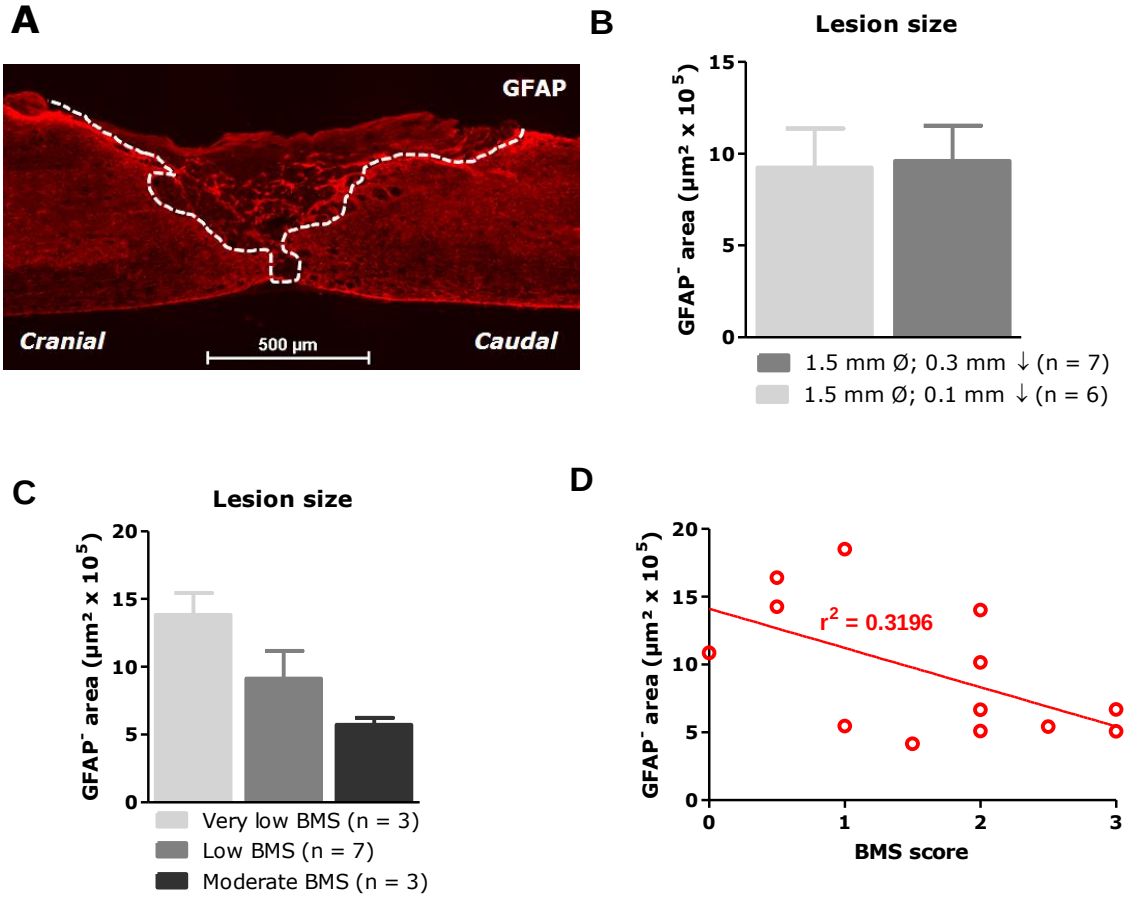

Figure 4: Correlation between BMS score and lesion size. Sections were stained for GFAP to determine the lesion size. The GFAP⁻ (A) area is delineated and measured with ImageJ software. Lesion size is analyzed according to impact depth (B) and locomotor recovery (BMS score) (C-D). Statistical analysis using the non-parametric Mann–Whitney U-test shows no difference between the two injury depths (↓) with the 1.5 mm tip diameter (Ø). Furthermore, animals with a very low BMS score (almost completely paralyzed) show the highest lesion size. On the other hand, animals with a moderate BMS score (plantar paw placement or dorsal stepping) show the lowest lesion size. However, analysis with the Kruskal-Wallis test shows no significant difference between the groups. Furthermore, the lesion size shows a moderate correlation ($r^2 = 0.3196$) with the BMS score ($p = 0.0493$). Very low BMS: a BMS score of 0 on one hindlimb and a score of 1 on the other. Low BMS: an average BMS score of 1 – 2. Moderate BMS: a BMS score of 3 on one hindlimb and a score of 2 or 3 on the other. Data represent Mean + SEM. GFAP: glial fibrillary acidic protein. BMS: Basso mouse scale.

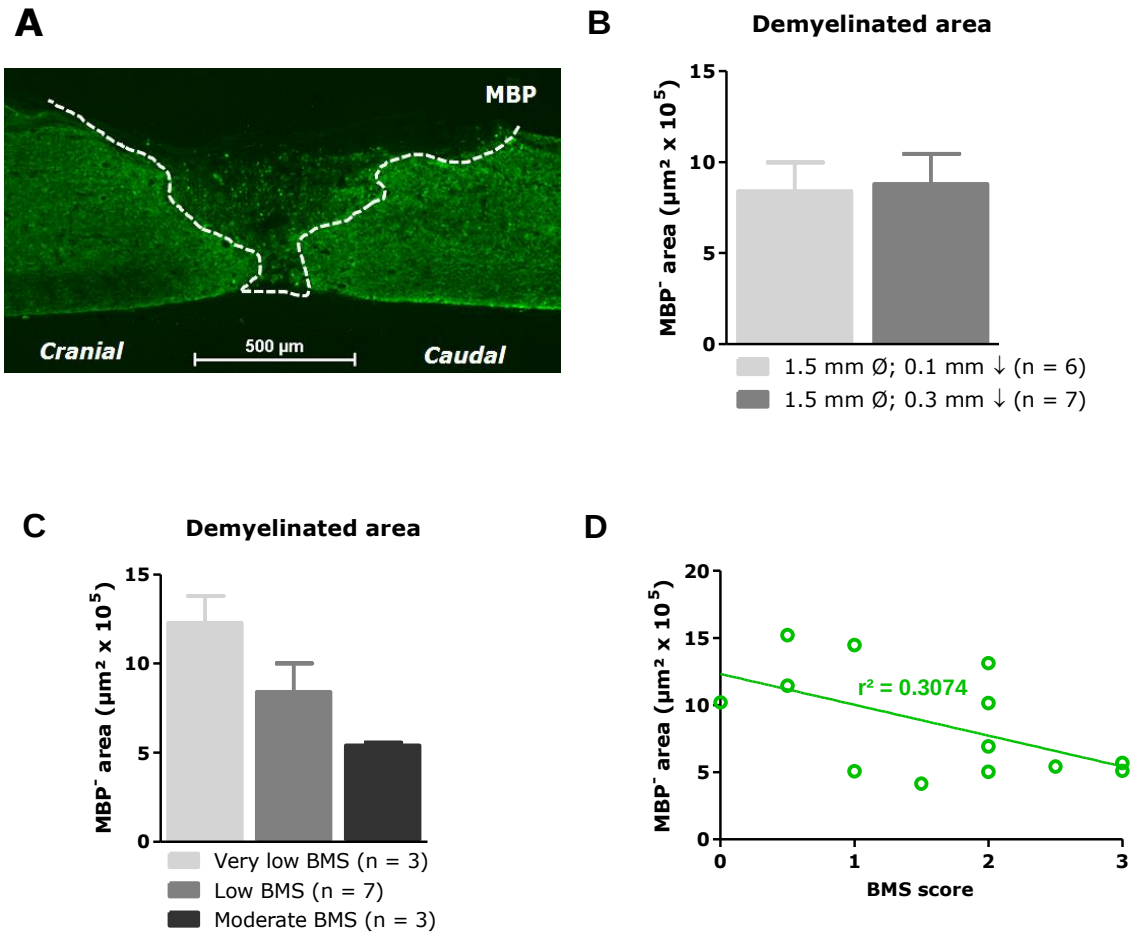

Figure 5: Correlation between BMS score and demyelinated area. Sections were stained for MBP to determine the demyelinated area. The MBP⁻ (A) area is delineated and measured with ImageJ. The demyelinated area is analyzed according to impact depth (B) and locomotor recovery (BMS score) (C). Statistical analysis using the non-parametric Mann–Whitney U-test shows no difference between the two injury depths (↓) with the 1.5 mm tip diameter (Ø). Furthermore, animals with a very low BMS score (almost completely paralyzed) show the highest demyelinated area. On the other hand, animals with a moderate BMS score (plantar paw placement or dorsal stepping) show the lowest demyelinated area. However, analysis with the Kruskal-Wallis test shows no significant difference between the groups. Furthermore, the demyelinated area shows a moderate correlation ($r^2 = 0.3074$) with the BMS score ($p = 0.0441$). Very low BMS: a BMS score of 0 on one hindlimb and a score of 1 on the other. Low BMS: an average BMS score of 1 – 2. Moderate BMS: a BMS score of 3 on one hindlimb and a score of 2 or 3 on the other. Data represent Mean + SEM. MBP: myelin basic protein. BMS: Basso mouse scale.

3.1.3 No significant difference in astrogliosis between the different injury groups

By measuring GFAP intensity 600 µm caudal and 600 µm cranial from the lesion side, the level of astrogliosis was analyzed (Figure 6A). No significant difference in astrogliosis was observed when animals were compared according to lesion depth (Figure 6B) or BMS score (Figure 6C).

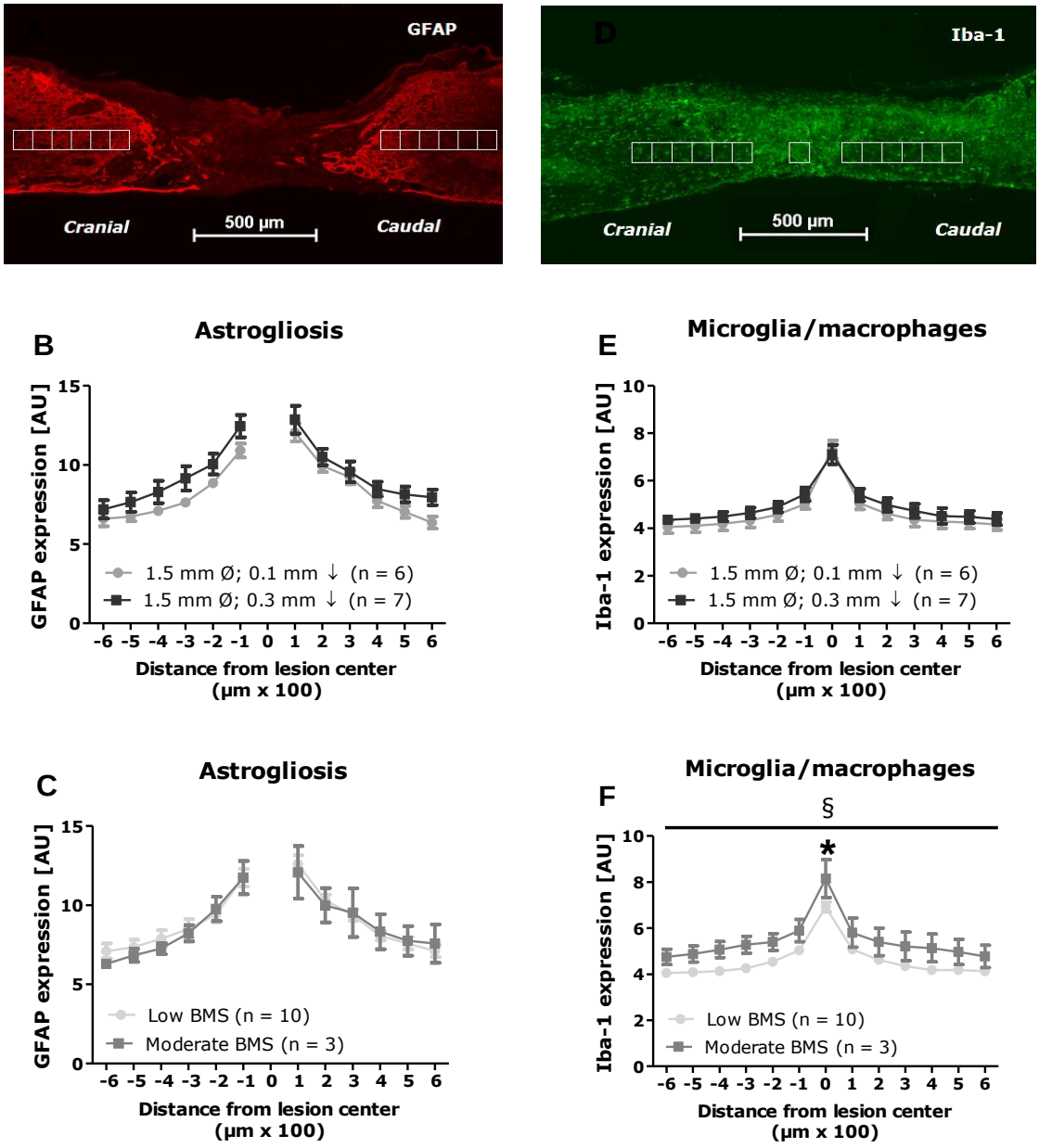

Figure 6: No difference in astrogliosis but significantly different microglia/macrophage infiltration in different injury groups. Sections were stained for GFAP and Iba-1 to determine the level of astrogliosis and microglia/macrophage infiltration. Quantification was performed via intensity analysis of GFAP (A) and Iba-1 (D) immunohistochemistry within square areas of 100 µm × 100 µm (white boxes) extending from 600 µm cranial to 600 µm caudal from the lesion site. In the Iba-1 stained sections, one additional measurement was performed in the middle of the lesion center. Analysis via two-way ANOVA for repeated measurements with the Bonferroni post-hoc test shows no difference in astrogliosis between different groups (B - C). Intensity analysis shows no significant difference in microglia/macrophage infiltration in lesions with different impact depths (↓) and a set tip diameter (Ø) of 1.5 mm (E). On the other hand, two-way ANOVA shows a significantly higher microglia/macrophage infiltration in animals with a moderate BMS score (plantar paw placement or dorsal stepping) compared to animals with a low BMS score (only ankle movement) (§). Bonferroni post-hoc test shows a significant difference at the lesion center only (*) (F). Low BMS: an average BMS score of 1 – 2. Moderate BMS: a BMS score of 3 on one hindlimb and a score of 2 or 3 on the other. Data represent mean ± SEM. * $p < 0.05$. § $p < 0.05$. GFAP: glial fibrillary acidic protein. Iba-1: ionized calcium-binding adapter molecule 1. BMS: Basso mouse scale.

3.1.4 Analysis of immune cell infiltration only reveals significant difference in microglia/macrophage infiltration between different injury groups.

To investigate the inflammatory response, immunohistochemistry was performed for the macrophage/microglia marker Iba-1 (Figure 6D–F) and the T helper cell marker CD4 (Figure 7). Additionally, an Oil red O staining was performed to analyze the amount of foamy macrophages in the injured spinal cords (Figure 8). Macrophage/microglia infiltration was analyzed by measuring Iba-1 intensity 600 µm caudal and 600 µm cranial from the lesion side with one additional measurement in the middle of the lesion (Figure 6D). Statistical analysis shows no significant difference between different injury depths (Figure 6E). On the other hand, two-way ANOVA shows significantly more macrophage/microglia spinal cords of animals with a better functional recovery (Figure 6F). Furthermore, after 3 weeks, the mean number of T helper cells per spinal cord section was not significantly different between different injury groups (Figure 7D). A weak negative correlation was observed between functional recovery and T helper cell infiltration (Figure 7E).

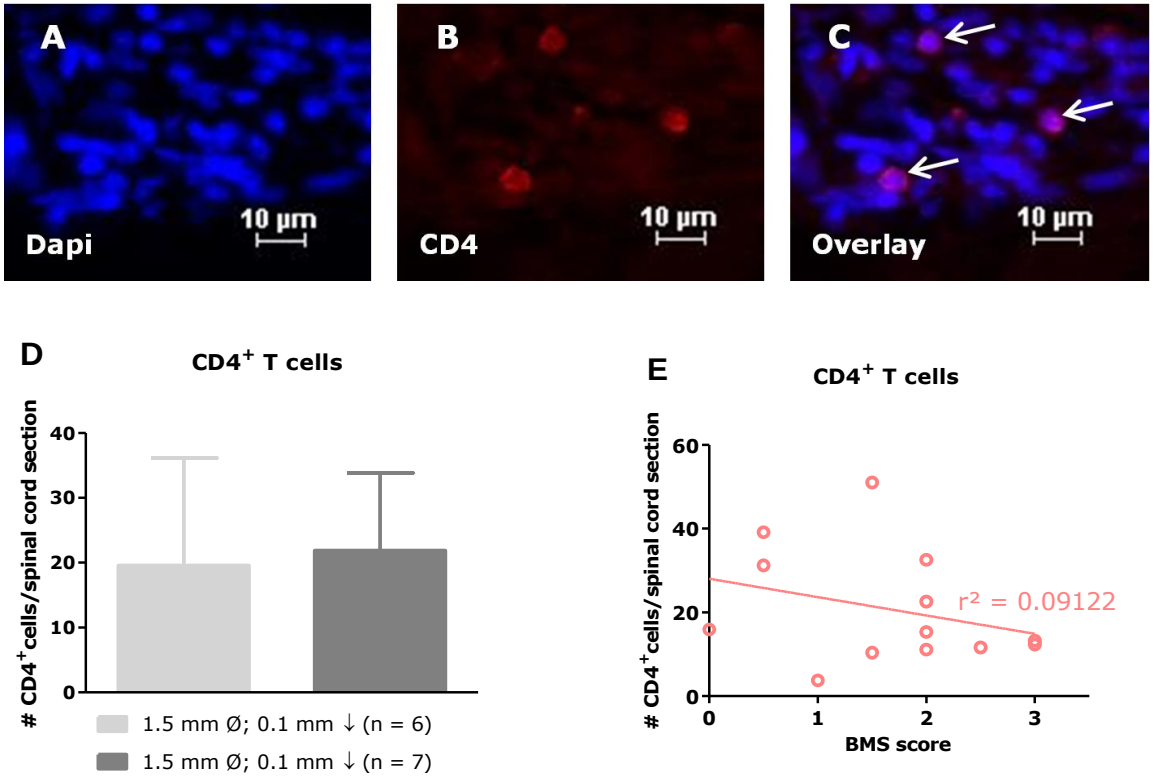

Figure 7: Weak negative correlation between the BMS score and T helper cell infiltration. Spinal cord sections were stained with CD4 to determine the level of T helper cell infiltration. Dapi staining is shown in panel A and CD4 staining in panel B. T helper cells are indicated by the white arrows (C). Statistical analysis using the non-parametric Mann–Whitney U-test shows no difference between the two injury depths (↓) with a set tip diameter (Ø) of 1.5 mm (D). Furthermore, there is a weak correlation (r^2 = 0.09122) between BMS score and the amount of $CD4^+$ T cells in the injured spinal cords (E). Data represent Mean + SEM. Dapi: 4',6-Diamidino-2-phenylindole. CD4: Cluster of differentiation 4. BMS: Basso mouse scale.

Furthermore, no significant difference in foamy macrophage infiltration was observed between the 0.1 mm and 0.3 mm groups but a weak negative correlation was observed between the BMS score and foamy macrophage infiltration. Animals with a higher functional recovery showed a lower amount of foamy macrophage infiltration compared to animals with a lower BMS score (Figure 8F). However, this correlation was not significant.

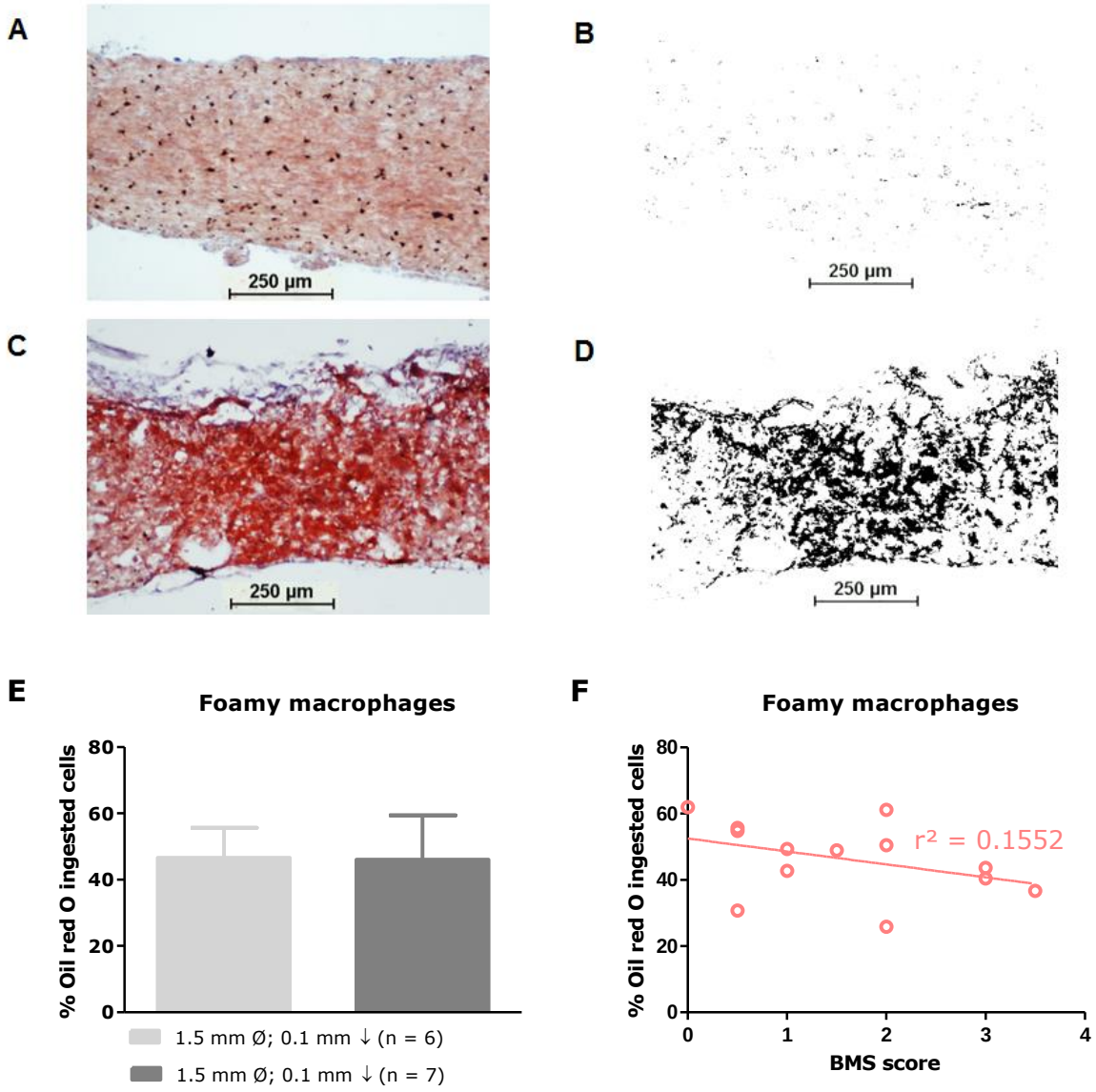

Figure 8: Weak negative correlation between the BMS score and foamy macrophage infiltration. Spinal cord sections were stained with Oil red O to determine the level of myelin ingested cells. An injured (C) and non-injured (A) spinal cord section stained with Oil red O is shown. Pixels with an intensity within the predetermined RGB threshold range are shown in black for an injured (B) and non-injured (D) spinal cord region. Statistical analysis using the non-parametric Mann–Whitney U-test shows no difference between the two injury depths (↓) at a set tip diameter (Ø) of 1.5 mm (E). Furthermore, there is a weak correlation (r^2 = 0.1552) between the BMS score and the amount of foamy macrophages in the injured spinal cords (F). Data represent Mean + SEM. BMS: Basso mouse scale.

3.2 Murine spinal cord contusion by a 1 mm tip and a 0.3 mm impact depth creates a moderate injury

3.2.1 Contusion injuries caused by a 1 mm tip and a 0.3 mm impact depth result in a moderate spontaneous functional recovery

Female Balb/c mice received a contusion SCI with a velocity 4.6 m/s, a dwell time of 500 ms and a tip diameter of 1 mm. Spontaneous functional recovery was measured via BMS scoring (Figure 9A). During the first 9 days, BMS scoring was performed daily. Additional measurements were performed on day 11, 13, 19 and 21. The group which received an injury with 0.1 mm impact depth shows an average BMS score of 5.2 after 1 week and an average score of 6.4 after 3 weeks. The group with an impact depth of 0.3 mm only shows an average BMS score of 2.3 after 1 week and an average score of 4 at 3 weeks post-injury. Furthermore, the rotarod performance test was used to analyze hindlimb motor coordination, balance and strength (Figure 9B). One week post-injury, all animals were able to use their hindlimbs on the rotarod performance test. In the 0.1 mm injury group, the average latency to fall at day 7 was 212 s. This increased to 297 s during the second week post-injury. Two weeks post-injury, only one animal was not able to stay on the rod for 300 s. In the 0.3 mm injury group the average latency to fall at day 7 was 140 s. This increased to 258 s during the second week post-injury. After 2 weeks, 3 out of 7 animals were able to stay on the rod for 300 s. Two-way ANOVA shows a significant difference between the two groups based on BMS scoring as well as on rotarod performance analysis.

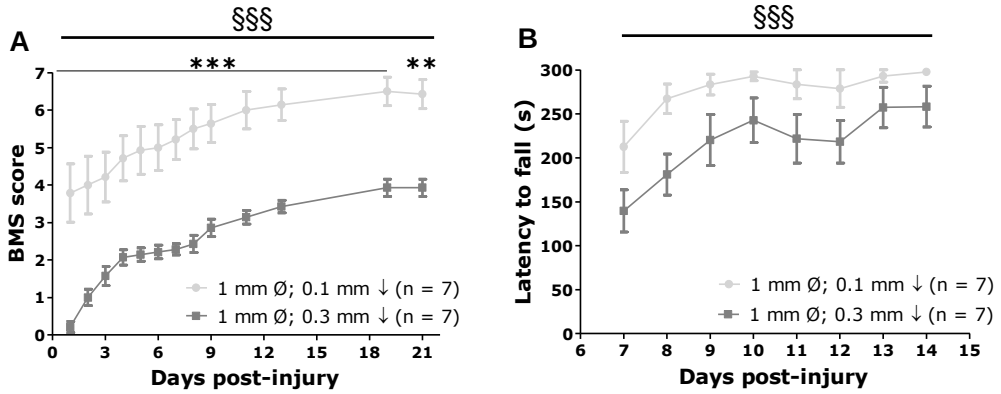

Figure 9: Contusion SCI by a 1 mm tip diameter and a 0.3 mm impact depth results in a moderate injury. Mice received a contusion SCI with an impactor tip diameter (Ø) of 1 mm. Two-way ANOVA shows a significant difference between the two injury depths (↓) at all time-points (§§§). Also Bonferroni post-hoc analysis indicates a significant difference at all time points (*** or **) The group which received an injury with 0.1 mm impact depth shows an average BMS score of 5.2 after 1 week and an average score of 6.4 after 3 weeks. The group with an impact depth of 0.3 mm only shows an average BMS score of 2.3 after 1 week and an average score of 4, 3 weeks post-injury (A). On the rotarod performance test, two-way ANOVA also showed a significant difference between the two injury groups (§§§). The average latency to fall at day 7 in the 0.1 mm injury group was 212 s. This increased to 297 s during the second week post-injury. In the 0.3 mm injury group the average latency to fall at day 7 was 140 s. This increased to 258 s during the second week post-injury (B). Data represent mean ± SEM. ** $p < 0.01$. *** $p < 0.001$. §§§ $p < 0.001$. BMS: Basso mouse scale.

3.2.2 Lesion size and demyelinated area are significantly higher after 0.3 mm impact depth compared to 0.1 mm injuries

The lesion size and demyelinated area were investigated in the different injury groups. Again, GFAP immunohistochemistry was used to evaluate the lesion size (Figure 10A) and MBP was used to investigate the level of demyelination (Figure 10B). Statistical analysis shows a significantly greater lesion size and demyelinated area in the injury group with an impact depth of 0.3 mm compared to the 0.1 mm group. As shown in representative images of the lesion center of the 0.1 mm (Figure 10C) and the 0.3 mm injury depth (Figure 10D), an obviously larger lesion size can be observed in spinal cords with an injury depth of 0.3 mm. Since the lesion size and the demyelinated area are comparable, only the lesion size is shown.

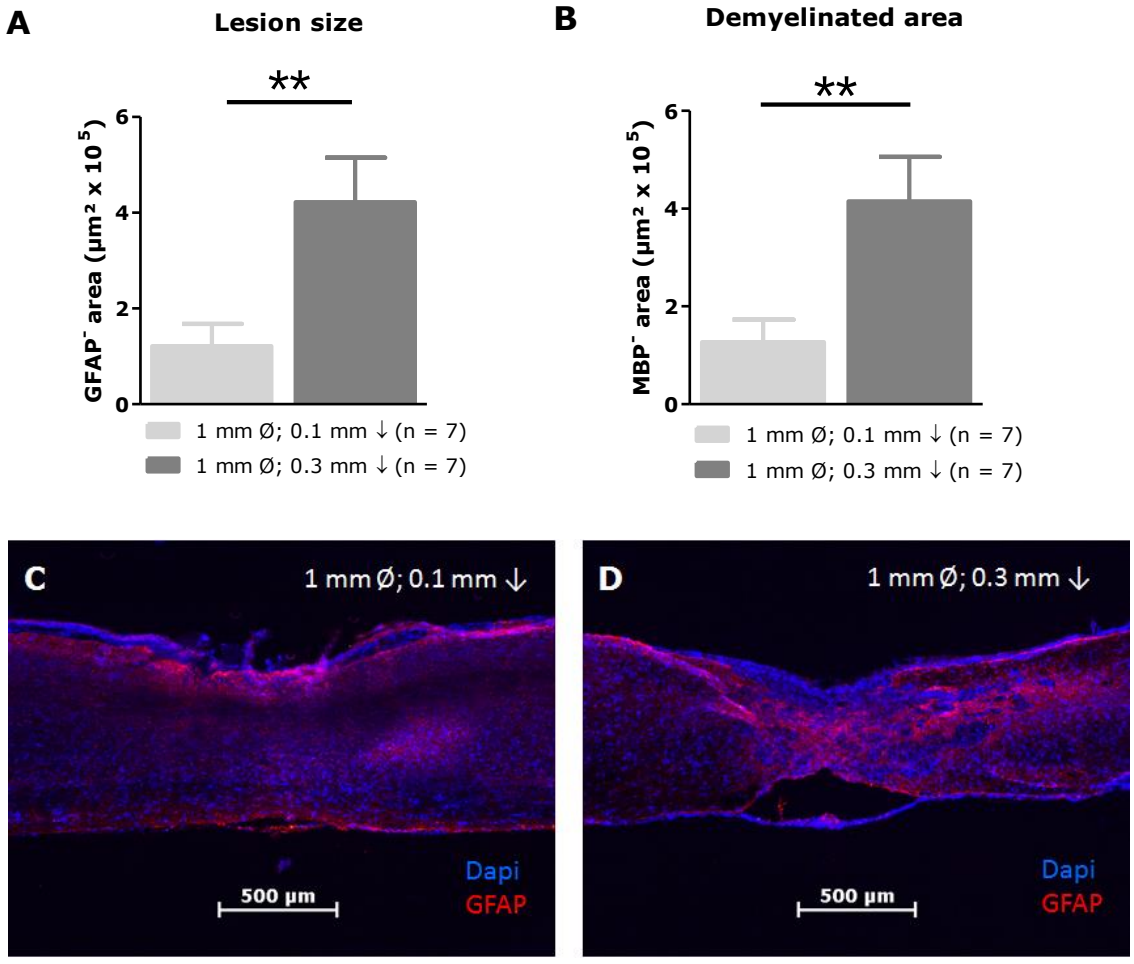

Figure 10: Lesion size and demyelinated area are significantly larger in the 0.3 mm injury depth group. Spinal cord sections were stained with GFAP and MBP to determine the lesion size and demyelinated area. Statistical analysis using the non-parametric Mann–Whitney U-test shows a significantly bigger lesion size (A) and demyelinated area (B) after a 0.3 mm injury depth (↓) (D) compared to a 0.1 mm injury depth (C), with a set tip diameter (Ø) of 1 mm. The MBP negative area is not shown since it is comparable to the GFAP negative area. Data represent Mean + SEM. GFAP: glial fibrillary acidic protein. MBP: myelin basic protein. Dapi: 4',6-Diamidino-2-phenylindole.

3.2.3 Astrogliosis is not significantly different between contusions with 0.1 mm and 0.3 mm injury depth

By measuring GFAP intensity 600 µm caudal and 600 µm cranial from the lesion side, the level of astrogliosis was analyzed. Statistical analysis shows no significant difference in astrogliosis between the different injury groups (Figure 11).

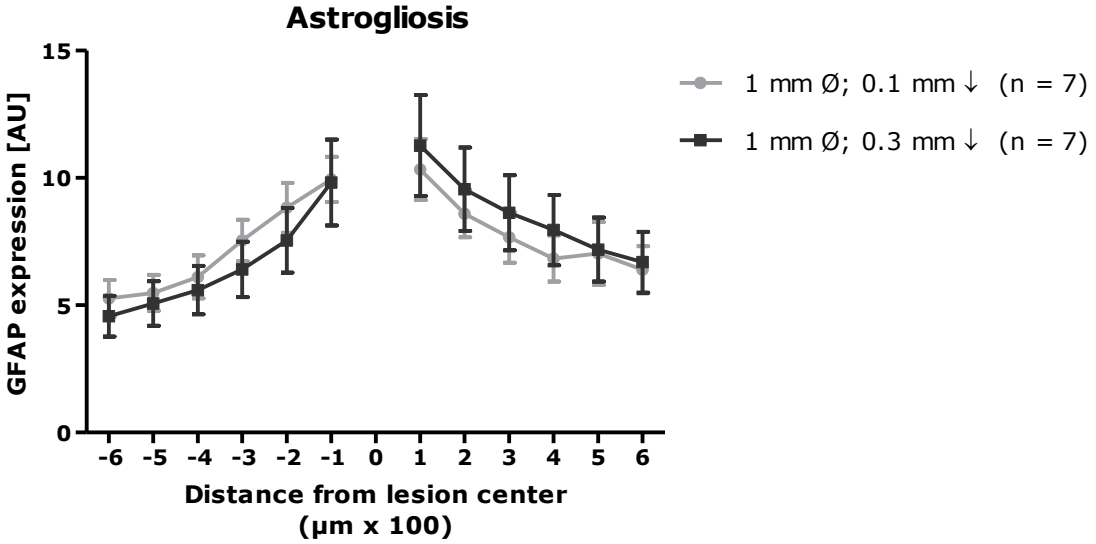

Figure 11: No difference in astrogliosis between 0.1 mm and 0.3 mm injury depth. Sections were stained for GFAP to determine the level of astrogliosis. Analysis via two-way ANOVA for repeated measurements with the Bonferroni post-hoc test shows no difference in astrogliosis between different injury depths (↓), with a set tip diameter (Ø) of 1 mm. Data represent mean ± SEM. GFAP: glial fibrillary acidic protein.

3.2.4 Increased microglia/macrophage and foamy macrophage activity in the 0.3 mm injury depth group

To investigate the inflammatory response, immunohistochemistry was performed for macrophage/microglia marker Iba-1 and T helper cell marker CD4. Furthermore, Oil red O was used to analyze the amount of foamy macrophages. Macrophage/microglia infiltration was analyzed by measuring Iba-1 intensity 600 µm caudal and 600 µm cranial as described previously. Two-way ANOVA shows significantly more macrophage/microglia in injuries with a bigger impact depth (Figure 12). Moreover, the amount of foamy macrophage activity is significantly higher in contusions with 0.3 mm injury depth compared to 0.1 mm injuries (Figure 13). In contrast, after 3 weeks, the mean number of T helper cells per spinal cord section was not significantly different between the different injury groups (Figure 14A). Interestingly, clusters of $CD4^+$ T cells were observed in contusions with a 1 mm tip diameter (Figure 14B-C).

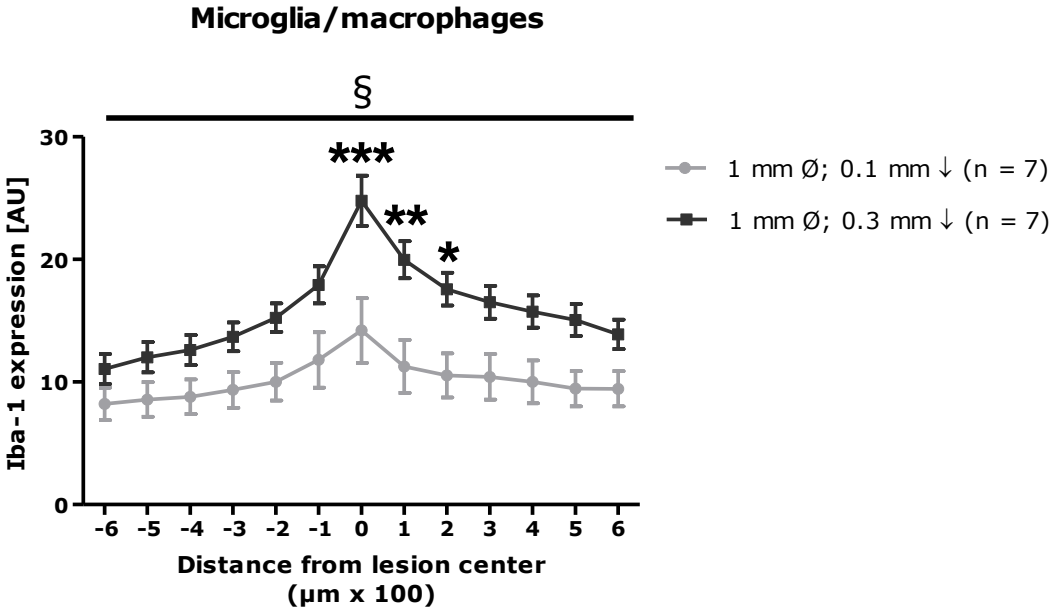

Figure 12: Significantly higher microglia/macrophage activation in contusions with 0.3 mm injury depth compared to 0.1 mm injuries. Sections were stained for Iba-1 to determine the level of microglia/macrophage infiltration. Quantification was performed via intensity analysis of Iba-1 immunohistochemistry. Analysis via two-way ANOVA for repeated measurements shows significantly higher microglia/macrophage infiltration in lesions with 0.3 mm depth compared to 0.1 mm, 3 weeks post-SCI (§). The Bonferroni post-hoc test indicates significant differences at the lesion center (***), 100 µm caudal (**) and 200 µm caudal (*) to the lesion center. Data represent mean ± SEM. * $p < 0.05$. ** $p < 0.01$. *** $p < 0.001$. § $p < 0.05$. Iba-1: ionized calcium-binding adapter molecule 1.

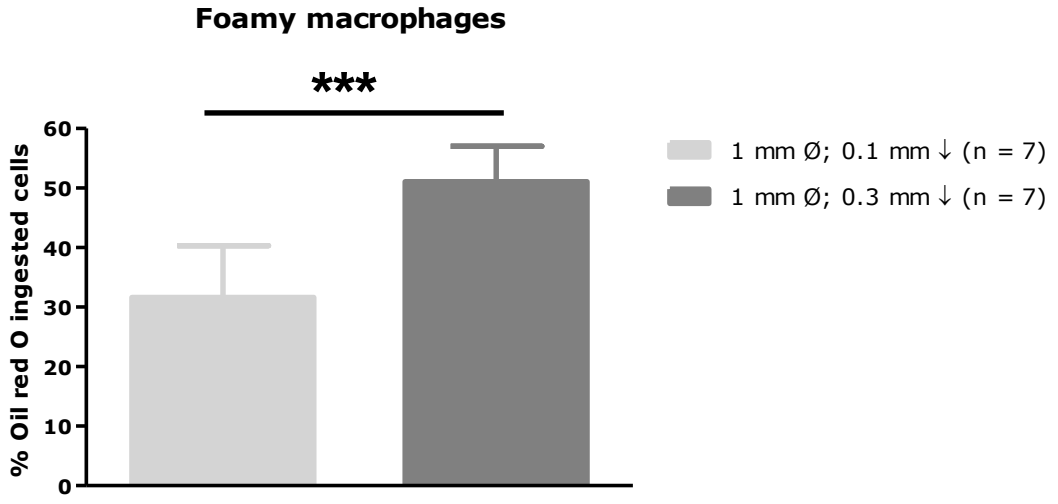

Figure 13: Significantly more foamy macrophage activity in contusions with a 0.3 mm injury depth compared to 0.1 mm injuries. Spinal cord sections were stained with Oil red O to determine the level of myelin ingested cells. Statistical analysis using the non-parametric Mann–Whitney U-test shows a significantly higher foamy macrophage activity in contusions with a 0.3 mm injury depth compared to 0.1 mm injuries. Data represent Mean + SEM. *** $p < 0.001$.

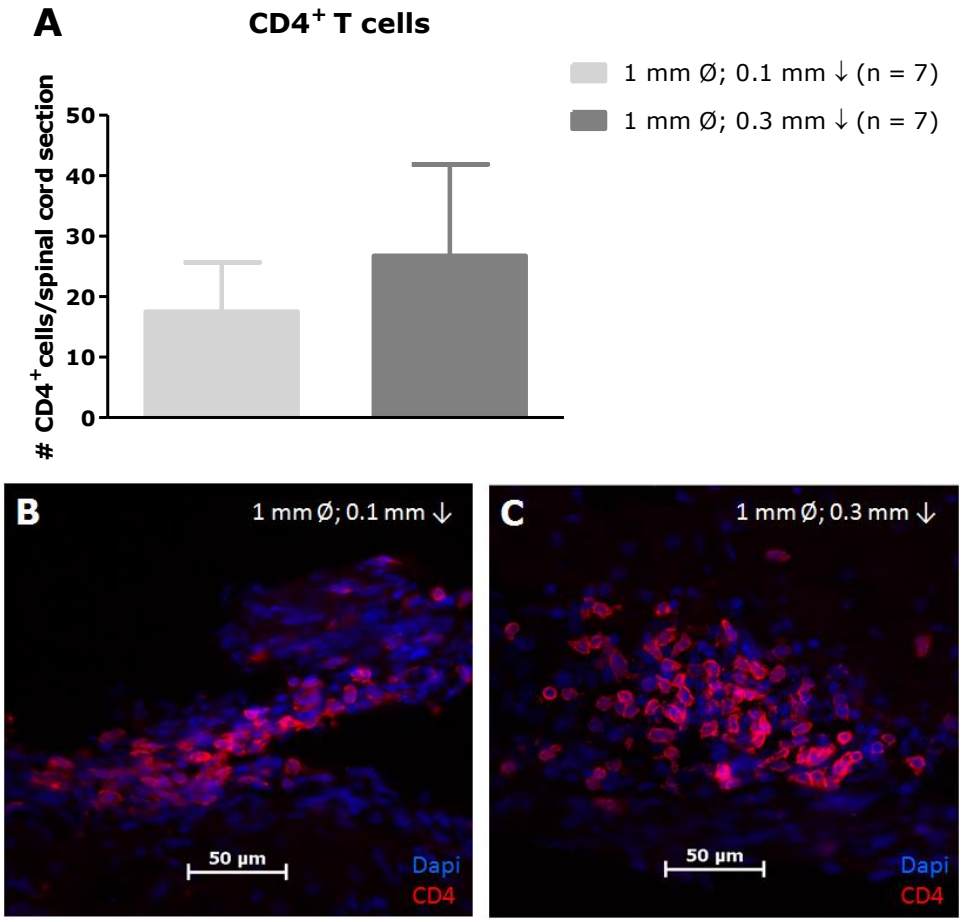

Figure 14: No significant difference in CD4$^+$ T cell infiltration between different injury groups. Spinal cord sections were stained with CD4 and manually counted to determine the level of T helper cell infiltration. Statistical analysis using the non-parametric Mann–Whitney U-test shows no difference between the two injury depths (A). Furthermore, clusters of CD4$^+$ T cells were observed in contusions with a 1 mm tip diameter and 0.1 mm (B) and 0.3 mm injury depth (C). Data represent Mean + SEM. CD4: Cluster of differentiation 4. Dapi: 4',6-Diamidino-2-phenylindole.

3.3 IL-13 improves functional recovery after contusion SCI

Female Balb/c mice received a contusion SCI with a CCI device using a velocity 4.6 m/s, a dwell time of 500 ms, a tip diameter of 1 mm and an impact depth of 0.3 mm. Furthermore, they were treated with IL-13 or PBS for 7 sequential days starting at day the day of surgery. Functional recovery was measured via BMS scoring (Figure 15A). Hindlimb motor coordination, balance and strength was measured via rotarod performance analysis (Figure 15B). During the first 7 days, BMS scoring was performed daily. Additional measurements were performed on day 9, 11, 13 and 15. Rotarod measurements were performed daily from day 7 until day 13 with one additional measurement on day 15. From day 3 on, the IL-13 treated group shows a significant treatment effect in functional recovery based on BMS scoring (§). The average BMS score on day 11 is 2.9 in the PBS-treated group, compared to 4.6 in the IL-13-treated group. These scores increase to 3.3 in the PBS group and 5.5 in the IL-13 group on day 15. On the rotarod performance test, a significant treatment effect of IL-13 was observed from day 7 on (§). In the PBS-treated group the average latency to fall at day 11 was 170.8 s, compared to 274.2 s in the IL-13-treated group. At day 13, all animals of the IL-13 group were able to stay on the rod for 300 s. At day 15, still all the IL-13 animals were able to stay on the rod for 300 s, while in the PBS group, the mean latency to fall of the rod was only 183 s.

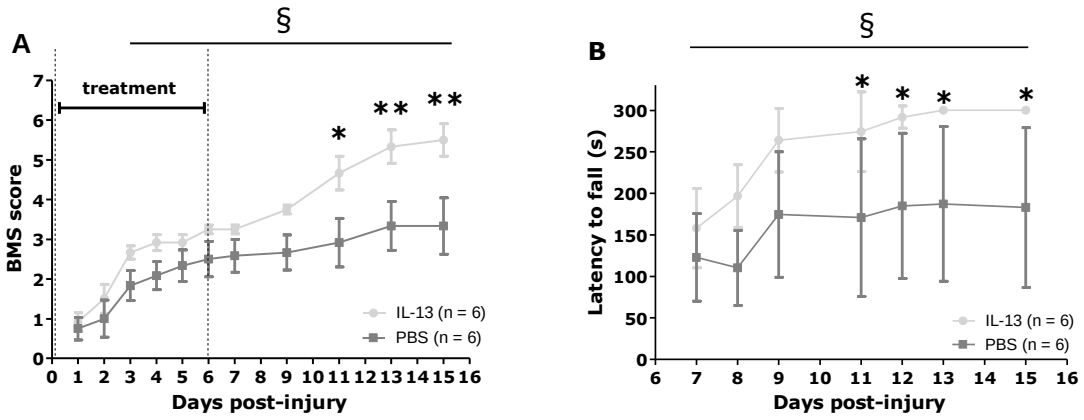

Figure 15: IL-13 improves functional recovery after contusion SCI. Mice received a contusion SCI with an impactor tip of 1 mm and an impact depth of 0.3 mm. Furthermore, they were treated with IL-13 or PBS for 7 sequential days starting at the day of surgery. Analysis of the BMS scores by two-way ANOVA shows a significant treatment effect between the two groups from day 3 on (§). Furthermore, a significant difference on individual time points is observed from day 11 on (* or **). The average BMS score on day 11 was 2.9 in the PBS-treated group, compared to 4.6 in the IL-13-treated group. These scores increase to 3.3 in the PBS group and 5.5 in the IL-13 group on day 15 (A). On the rotarod performance test, two-way ANOVA shows a significant treatment effect (§) between the two groups from day 11 on. The Bonferroni post-hoc test shows a significant difference on individual time points (*). In the PBS-treated group the average latency to fall at day 11 was 170.8 s, compared to 274.2 s in the IL-13-treated group. From day 13 on, all animals of the IL-13 treated group were able to stay on the rod. After 15 days, the PBS group was able to stay on the rod for 183 s (B). Data represent mean ± SEM. * $p < 0.05$. ** $p < 0.01$. § $p < 0.05$. BMS: Basso mouse scale. IL-13: interleukin-13. PBS: phosphate buffered saline.

4. Discussion

Currently, there is no fully restorative therapy available for SCI patients. Therefore, the use of representative disease models in which therapeutic options can be investigated is needed. Essential in SCI research is the use of animal models, different models are widely used to study different aspects of this condition. In this study, the focus lies on the optimization of the contusion SCI model at our research facility and the implementation by testing the therapeutic potential of IL-13.

A *good* animal model in scientific research is defined as a standardized, reproducible model, which also resembles the clinical situation in humans (32). Furthermore, a small variation in the outcome measures is an essential feature of a well-standardized model. The currently used SCI model at our research facility is the hemisection model. This is a good model to study axon regeneration since important motor tracts in the spinal cord, e.g. the corticospinal tract, are transected. Unfortunately, this model does not give a complete representation of all the clinical aspects of SCI in humans. Therefore, a contusion SCI model is established at our research facility.

A moderate contusion model was chosen since it shows a certain degree of spontaneous functional recovery. This way, animals have room to functionally improve with a potential therapy. In our study, the animal model was established when the animals show spontaneous recovery in which plantar paw placement, dorsal stepping or occasional plantar stepping was accomplished, 3 weeks post-injury. This degree of functional recovery correlates with a BMS score of 3 or 4. In most cases, there is a correlation between the BMS score and the spinal cord histology after injury. This was observed in several studies with contusion models in rodents. For example, functional recovery correlates with grey and white matter tissue sparing and the overall lesion size negatively correlates with functional outcome (33-37). Moreover, functional recovery partly depends on the extent of inflammation in the injured spinal cord after contusion SCI (33). After the model was established, IL-13 was tested as a therapeutic option for SCI via systemic administration in the contusion injury mouse model.

In the first contusion experiment, an impact diameter of 1 mm was tested with an impact depth of 0.1 mm, 0.3 mm or 0.5 mm (Figure S1). The survival rate of this experiment was 37.5%. One possible explanation of this high mortality is an unruptured dura in most of the contusion injuries with a low impact depth. This causes spreading of blood and tissue liquids underneath the dura surface, which leads to an increased pressure on the spinal cord and the brain, eventually killing the animals (38). In the following experiments, the dura was punctured with a thin needle after the contusion injury was inflicted.

After puncturing the dura in a following experiment, the survival rate increased to 58%. The unruptured dura in the first 1 mm tip experiment might have worsened the injury of the low impact depth group via an increased pressure on the spinal cord caused by the bleeding underneath the dura surface. This way, no clear difference could be observed between the 0.1 mm and 0.3 mm injury depths. The BMS score of the 1 mm tip diameter; 0.3 mm impact depth group resembles the scores observed in other moderate contusion injury models in Balb/c mice (13, 39). The BMS scores allow room for improvement with a potential therapy. Moreover, the small error bars show a

small variation in this injury group, which is a requirement for a good animal model. The 1.5 mm tip injuries, on the other hand, result in a severe contusion injury consistent with literature findings (13).

Next, lesion characteristics were evaluated via histological analysis of the injured tissue. In a contusion injury, the initial damage is induced by the contusion of the spinal cord. This damage is smaller compared to the damage observed in the hemisection model. On the other hand, the secondary injury is much more pronounced in contusion injuries. This secondary injury consists of a cascade of injury-induced destructive events that spread in a rostrocaudal matter, which causes further loss of function (34). The lesion size and demyelinated area are bigger in the more severely injured spinal cords compared to the less injured spinal cords. This can be explained by the damage that occurs during these secondary injury processes, which are characterized by neuronal and axonal destruction and demyelination. Furthermore, pro-inflammatory cytokines contribute to the death of neurons and oligodendrocytes (6, 8, 9). The results indicate that the lesion size and demyelinated area correlate with functional outcome. This is consistent with other studies concerning moderate contusions in female Balb/c mice (13, 39).

Furthermore, the inflammatory response was analyzed. The infiltration of $CD4^+$ T cells and the activity of microglia/macrophages, and more specifically foamy macrophages was measured in the injured spinal cords. A more pronounced inflammatory response may result in a further reduction in functional outcome due to scar tissue development and necrosis or apoptosis of neurons and oligodendrocytes. However, also a potentially beneficial role of the inflammatory after contusion SCI have been reported. This indicates a dual nature of inflammation after SCI (34).

Within both the 1.5 mm and 1 mm tip diameter group, a higher number of $CD4^+$ cells was present in the spinal cord of animals with a lower functional recovery, indicating a mild negative correlation between BMS score and $CD4^+$ T cell infiltration. Animals that are more severely injured and show poorer functional recovery, probably suffer from a more pronounced immune response in which more $CD4^+$ activation is present. Moreover, clusters of $CD4^+$ cells were observed in both 1 mm tip diameter groups. Since Balb/c mice are a Th2 dominated strain, it may be possible that these clusters consist of Th2 $CD4^+$ cells. These anti-inflammatory $CD4^+$ cells may elicit a protective T-cell response (40). This may also contribute to the higher functional recovery compared to the 1.5 mm tip diameter groups.

Both Th1 and, to a greater extent, Th2 cells can support neuroprotection and neuroregeneration. In entorhinal-hippocampal brain slice cultures from mice, Th1 as well as Th2 cells were capable of supporting neuronal survival. However, Th2 cells elicited higher protective effects compared to Th1 cells (41). Furthermore, evidence shows that a shift from Th1 to Th2 may further increase neuroprotection and axon regeneration and improve functional outcome after CNS injury. For example, inducers of a systemic Th2 switch, such as statins and -glatiramer acetate, can support either neuroprotection or regeneration, or both (42, 43).

Next, the microglia/macrophage activity was analyzed in the injured spinal cord. Chronic inflammation is a hallmark of contusion SCI in which microglia and macrophages dominate the

lesion site (10). In both the 1 mm and 1.5 mm tip diameter injury groups, more microglia/macrophages were observed in the 0.3 mm injury depth compared to the 0.1 mm depth. This is consistent with the hypothesis that microglia/macrophages play a detrimental role in SCI. A more severe injury can elicit a more severe immune reaction accompanied by an increased activation of microglia/macrophages. CNS macrophages can contribute to a decreased functional recovery and their depletion or inhibition can aid in neuroprotection (44, 45). The M1 macrophages that dominate the lesion site after SCI impair recovery via spreading of secondary neurodegenerative cascades and stimulating retraction of axons at the site of injury (46). These M1 macrophages can release cytokines, reactive oxygen species, proteolytic enzymes and nitric oxide, which are capable of killing neurons and glia (47).

On the other hand, activation or augmentation of CNS macrophages can enhance CNS repair. For example, CNS macrophages can contribute to axon growth, axon sprouting, remyelination, and perhaps long-distance regeneration (48, 49). In the 1.5 mm tip diameter groups, more microglia/macrophages were present in the lesion center of animals with a better functional recovery, 3 weeks post-injury. Furthermore, CNS macrophages may protect and/or repair nerves via the modulation of glutamate excitotoxicity. Microglia/macrophages can increase glutamate transporters and, in this way, increase extracellular glutamate uptake (50, 51). The potential to promote nerve regeneration was demonstrated in a model for optic nerve injury. Activated macrophages were able to release a protein called oncomodulin, which was responsible for promoting regeneration of injured retinal ganglion cells (52). However, this process also leads to the release of neurotoxic molecules (53).

In the injured CNS, increased entrance of hematogenous macrophages and increased phagocytic activity of resident microglia might lead to more efficient clearance of the degenerating CNS myelin, leading to a better functional recovery. It has been observed that microglia/macrophages derived from monocytes play an important role in tissue repair (18, 54). This occurs in part via the induction of scavenger receptors and matrix degrading enzymes which can enhance phagocytosis and promote tissue remodeling (55, 56).

Lipid accumulation in the spinal cord lesion due to myelin degeneration leads to the formation of foamy macrophages and lipid plaques. These foamy macrophages originate from M2 macrophages that have lost their M2 phenotype and took on foamy cell characteristics after myelin ingestion. The effect of myelin on the inflammatory state of these macrophages is still under debate (57). Studies have reported a pro-inflammatory phenotype with a role in enhancing neurotoxicity, impairing wound healing and maintaining the chronic inflammatory response (58). However, other studies show that these myelin-ingested macrophages obtain an anti-inflammatory phenotype (59).

The higher amount of macrophages observed with a higher BMS score in the 1.5 mm tip experiment is not due to the presence of foamy macrophages. The BMS score showed a mild negative correlation with foamy macrophage activity. Furthermore, a higher amount of foamy macrophages was observed in contusions with a deeper injury in the 1 mm tip diameter experiment. These injuries also have an increased lesion size and demyelinated area, which need to be cleaned by foamy macrophages.

In the second phase of this study, the therapeutic potential of IL-13 was investigated in the contusion SCI mouse model using the parameters optimized in the first phase. In this experiment, all animals were anesthetized using isoflurane, which led to a survival rate of 90%. The therapeutic potential of IL-13 had already been tested by our group in the hemisection mouse model using the same treatment protocol (Figure S2). In this model, a significant treatment effect was observed from day 7 on. In the contusion SCI model, a significant treatment effect of IL-13 is already observed 3 days post-SCI. This earlier observed treatment effect may be due to the fact that the contusion model is better suited to study the secondary pathogenesis of SCI compared to the hemisection model. Since IL-13 acts upon the secondary pathology, this may explain why the treatment effect is observed sooner in the contusion model. This treatment effect can be due to the stimulation of a shift from type 1 to type 2 immunity via an IL-13 mediated mechanism (9).

It is known from the literature that IL-13 can suppress the production of anti-inflammatory mediators produced by microglia *in vitro* and *in vivo* (60, 61). Furthermore, IL-13 has an inhibitory function on MBP-directed T cell or B cell immunoreactivity *in vitro* and *in vivo*, in experimental autoimmune encephalomyelitis (EAE) (62). Moreover, IL-13 plays a role in the reversal of clinical signs of EAE via the suppression of type 1-mediated autoimmune responses (63).

In a later phase, the histology of the spinal cord tissue must be evaluated. We expect the lesion size and demyelinated area to be reduced in the treated spinal cords but this is to be investigated. Moreover, this is not a necessity to show functional improvement. Significant differences concerning the immune reaction are more likely to be observed. The IL-13 treatment might lead to a less severe immune reaction in the spinal cord tissue.

Besides determining immune cell numbers, the activation status or immune cell phenotype must also be explored. We anticipate that there will be more type 2 immune cells present compared to the amount of type 1 cells after IL-13 treatment. This is accompanied with a shift from Th1 and M1 to Th2 and M2, leading to a more anti-inflammatory environment (6, 8, 9).

Conclusively, IL-13 can be used as a therapeutic option for SCI in mice. Further studies are required before practical application of IL-13 in clinical settings. However, this study already shows promising perspectives for future therapies.

5. Conclusion

The goal of this study was to establish a contusion mouse model for SCI and to investigate the therapeutic potential of IL-13 in this clinically relevant model. By testing different parameter-combinations, a mouse model for contusion SCI is implemented at our research facility. A moderate contusion model with small variation was obtained by using a velocity of 4.6 m/s, a dwell time of 500 ms, a tip diameter of 1 mm and an impact depth of 0.3 mm.

Furthermore, preliminary data from our research team had shown previously a therapeutic potential of IL-13 after hemisection SCI. This study shows that IL-13 can also significantly improve functional recovery in the contusion model for SCI. Histological analysis of spinal cords from animals that have been treated with IL-13 after contusion SCI might help to unravel underlying mechanisms of IL-13 in the secondary pathology of SCI.

Lastly, this contusion model can now be used by our group in addition to the hemisection model to study other treatment options for SCI. Moreover, different aspects of the condition can be investigated by means of this model. For example, it may be useful to gain more understanding of the molecular mechanisms that drive the immune response towards a type 1 phenotype after SCI. In this way, new therapeutic targets might be discovered to switch the immune response from a type 1 to a type 2 phenotype in the recovery of SCI (18).

References

1. Singh A, Tetreault L, Kalsi-Ryan S, Nouri A, Fehlings MG. Global prevalence and incidence of traumatic spinal cord injury. Clin Epidemiol. 2014;6:309-31.
2. Maynard FM, Bracken MB, Creasey G, Ditunno JF, Donovan WH, Ducker TB, et al. International Standards for Neurological and Functional Classification of Spinal Cord Injury. American Spinal Injury Association. Spinal Cord. 1997;35(5):266-74.
3. Ditunno JF, Young W, Donovan WH, Creasey G. The international standards booklet for neurological and functional classification of spinal cord injury. American Spinal Injury Association. Paraplegia. 1994;32(2):70-80.
4. Lee BB, Cripps RA, Fitzharris M, Wing PC. The global map for traumatic spinal cord injury epidemiology: update 2011, global incidence rate. Spinal Cord. 2014;52(2):110-6.
5. Singh R, Rohilla R, Siwach R, Dhankar S, Kaur K. Understanding Psycho-Social Issues in Persons with Spinal Cord Injury and Impact of Remedial Measures. Int j psychosoc rehabil. 2012;16(1):95-100.
6. Macaya D, Spector M. Injectable hydrogel materials for spinal cord regeneration: a review. Biomed Mater. 2012;7(1):012001.
7. Thuret S, Moon LD, Gage FH. Therapeutic interventions after spinal cord injury. Nat Rev Neurosci. 2006;7(8):628-43.
8. Zhou X, He X, Ren Y. Function of microglia and macrophages in secondary damage after spinal cord injury. Neural Regen Res. 2014;9(20):1787-95.
9. Vidal PM, Lemmens E, Dooley D, Hendrix S. The role of "anti-inflammatory" cytokines in axon regeneration. Cytokine Growth Factor Rev. 2013;24(1):1-12.
10. Donnelly DJ, Popovich PG. Inflammation and its role in neuroprotection, axonal regeneration and functional recovery after spinal cord injury. Exp Neurol. 2008;209(2):378-88.
11. Rolls A, Shechter R, Schwartz M. The bright side of the glial scar in CNS repair. Nat Rev Neurosci. 2009;10(3):235-41.
12. Gaudet AD, Popovich PG, Ramer MS. Wallerian degeneration: gaining perspective on inflammatory events after peripheral nerve injury. J Neuroinflammation. 2011;8:110.
13. Ghasemlou N, Kerr BJ, David S. Tissue displacement and impact force are important contributors to outcome after spinal cord contusion injury. Exp Neurol. 2005;196(1):9-17.
14. Jun C, C. XZ, Xiao-Ming X, H. ZJ. Animal models of acute neurological injuries. Springer, editor. Totowa: Humana Press; 2009. 447 p.
15. Streijger F, Beernink TM, Lee JH, Bhatnagar T, Park S, Kwon BK, et al. Characterization of a cervical spinal cord hemicontusion injury in mice using the infinite horizon impactor. J Neurotrauma. 2013;30(10):869-83.
16. Boato F, Rosenberger K, Nelissen S, Geboes L, Peters EM, Nitsch R, et al. Absence of IL-1beta positively affects neurological outcome, lesion development and axonal plasticity after spinal cord injury. J Neuroinflammation. 2013;10:6.
17. Schwartz M, Hauben E. T cell-based therapeutic vaccination for spinal cord injury. Prog Brain Res. 2002;137:401-6.
18. Kigerl KA, Gensel JC, Ankeny DP, Alexander JK, Donnelly DJ, Popovich PG. Identification of two distinct macrophage subsets with divergent effects causing either neurotoxicity or regeneration in the injured mouse spinal cord. J Neurosci. 2009;29(43):13435-44.
19. Hershey GK. IL-13 receptors and signaling pathways: an evolving web. J Allergy Clin Immunol. 2003;111(4):677-90; quiz 91.
20. Gordon S, Martinez FO. Alternative activation of macrophages: mechanism and functions. Immunity. 2010;32(5):593-604.

21. Hallett MA, Venmar KT, Fingleton B. Cytokine stimulation of epithelial cancer cells: the similar and divergent functions of IL-4 and IL-13. Cancer Res. 2012;72(24):6338-43.
22. Schwartz M. "Tissue-repairing" blood-derived macrophages are essential for healing of the injured spinal cord: from skin-activated macrophages to infiltrating blood-derived cells? Brain Behav Immun. 2010;24(7):1054-7.
23. Matsukawa A, Hogaboam CM, Lukacs NW, Lincoln PM, Evanoff HL, Strieter RM, et al. Expression and contribution of endogenous IL-13 in an experimental model of sepsis. J Immunol. 2000;164(5):2738-44.
24. Rossi S, Mancino R, Bergami A, Mori F, Castelli M, De Chiara V, et al. Potential role of IL-13 in neuroprotection and cortical excitability regulation in multiple sclerosis. Mult Scler. 2011;17(11):1301-12.
25. Yang MS, Park EJ, Sohn S, Kwon HJ, Shin WH, Pyo HK, et al. Interleukin-13 and -4 induce death of activated microglia. Glia. 2002;38(4):273-80.
26. Shin WH, Lee DY, Park KW, Kim SU, Yang MS, Joe EH, et al. Microglia expressing interleukin-13 undergo cell death and contribute to neuronal survival in vivo. Glia. 2004;46(2):142-52.
27. Nelissen S, Vangansewinkel T, Geurts N, Geboes L, Lemmens E, Vidal PM, et al. Mast cells protect from post-traumatic spinal cord damage in mice by degrading inflammation-associated cytokines via mouse mast cell protease 4. Neurobiol Dis. 2014;62:260-72.
28. Hiruma S, Otsuka K, Satou T, Hashimoto S. Simple and reproducible model of rat spinal cord injury induced by a controlled cortical impact device. Neurol Res. 1999;21(3):313-23.
29. Basso DM, Fisher LC, Anderson AJ, Jakeman LB, McTigue DM, Popovich PG. Basso Mouse Scale for locomotion detects differences in recovery after spinal cord injury in five common mouse strains. J Neurotrauma. 2006;23(5):635-59.
30. Sheng H, Wang H, Homi HM, Spasojevic I, Batinic-Haberle I, Pearlstein RD, et al. A no-laminectomy spinal cord compression injury model in mice. J Neurotrauma. 2004;21(5):595-603.
31. Wu J, Renn CL, Faden AI, Dorsey SG. TrkB.T1 contributes to neuropathic pain after spinal cord injury through regulation of cell cycle pathways. J Neurosci. 2013;33(30):12447-63.
32. Lemmon VP, Ferguson AR, Popovich PG, Xu XM, Snow DM, Igarashi M, et al. Minimum information about a spinal cord injury experiment: a proposed reporting standard for spinal cord injury experiments. J Neurotrauma. 2014;31(15):1354-61.
33. Hillard VH, Peng H, Zhang Y, Das K, Murali R, Etlinger JD, et al. Tempol, a nitroxide antioxidant, improves locomotor and histological outcomes after spinal cord contusion in rats. J Neurotrauma. 2004;21(10):1405-14.
34. Hausmann ON. Post-traumatic inflammation following spinal cord injury. Spinal Cord. 2003;41(7):369-78.
35. Jeong MA, Plunet W, Streijger F, Lee JH, Plemel JR, Park S, et al. Intermittent fasting improves functional recovery after rat thoracic contusion spinal cord injury. J Neurotrauma. 2011;28(3):479-92.
36. Nishi RA, Liu H, Chu Y, Hamamura M, Su MY, Nalcioglu O, et al. Behavioral, histological, and ex vivo magnetic resonance imaging assessment of graded contusion spinal cord injury in mice. J Neurotrauma. 2007;24(4):674-89.
37. Pajoohesh-Ganji A, Byrnes KR, Fatemi G, Faden AI. A combined scoring method to assess behavioral recovery after mouse spinal cord injury. Neurosci Res. 2010;67(2):117-25.
38. Joost V, Elly H, Inge H, Jan W, Arthur B, Gerard B, et al. Neurotherapy: Progress in Restorative Neuroscience and Neurology. Oxford: Elsevier; 2009. 529 p.
39. Lopez-Vales R, Redensek A, Skinner TA, Rathore KI, Ghasemlou N, Wojewodka G, et al. Fenretinide promotes functional recovery and tissue protection after spinal cord contusion injury in mice. J Neurosci. 2010;30(9):3220-6.
40. Hendrix S, Nitsch R. The role of T helper cells in neuroprotection and regeneration. J Neuroimmunol. 2007;184(1-2):100-12.
41. Wolf SA, Fisher J, Bechmann I, Steiner B, Kwidzinski E, Nitsch R. Neuroprotection by T-cells depends on their subtype and activation state. J Neuroimmunol. 2002;133(1-2):72-80.

42. Lu D, Goussev A, Chen J, Pannu P, Li Y, Mahmood A, et al. Atorvastatin reduces neurological deficit and increases synaptogenesis, angiogenesis, and neuronal survival in rats subjected to traumatic brain injury. J Neurotrauma. 2004;21(1):21-32.
43. Pannu R, Barbosa E, Singh AK, Singh I. Attenuation of acute inflammatory response by atorvastatin after spinal cord injury in rats. J Neurosci Res. 2005;79(3):340-50.
44. Popovich PG, Guan Z, Wei P, Huitinga I, van Rooijen N, Stokes BT. Depletion of hematogenous macrophages promotes partial hindlimb recovery and neuroanatomical repair after experimental spinal cord injury. Exp Neurol. 1999;158(2):351-65.
45. Saville LR, Pospisil CH, Mawhinney LA, Bao F, Simedrea FC, Peters AA, et al. A monoclonal antibody to CD11d reduces the inflammatory infiltrate into the injured spinal cord: a potential neuroprotective treatment. J Neuroimmunol. 2004;156(1-2):42-57.
46. Horn KP, Busch SA, Hawthorne AL, van Rooijen N, Silver J. Another barrier to regeneration in the CNS: activated macrophages induce extensive retraction of dystrophic axons through direct physical interactions. J Neurosci. 2008;28(38):9330-41.
47. Block ML, Zecca L, Hong JS. Microglia-mediated neurotoxicity: uncovering the molecular mechanisms. Nat Rev Neurosci. 2007;8(1):57-69.
48. Vallieres N, Berard JL, David S, Lacroix S. Systemic injections of lipopolysaccharide accelerates myelin phagocytosis during Wallerian degeneration in the injured mouse spinal cord. Glia. 2006;53(1):103-13.
49. Barrette B, Hebert MA, Filali M, Lafortune K, Vallieres N, Gowing G, et al. Requirement of myeloid cells for axon regeneration. J Neurosci. 2008;28(38):9363-76.
50. Rimaniol AC, Haik S, Martin M, Le Grand R, Boussin FD, Dereuddre-Bosquet N, et al. Na+-dependent high-affinity glutamate transport in macrophages. J Immunol. 2000;164(10):5430-8.
51. van Landeghem FK, Stover JF, Bechmann I, Bruck W, Unterberg A, Buhrer C, et al. Early expression of glutamate transporter proteins in ramified microglia after controlled cortical impact injury in the rat. Glia. 2001;35(3):167-79.
52. Yin Y, Henzl MT, Lorber B, Nakazawa T, Thomas TT, Jiang F, et al. Oncomodulin is a macrophage-derived signal for axon regeneration in retinal ganglion cells. Nat Neurosci. 2006;9(6):843-52.
53. Yin Y, Cui Q, Li Y, Irwin N, Fischer D, Harvey AR, et al. Macrophage-derived factors stimulate optic nerve regeneration. J Neurosci. 2003;23(6):2284-93.
54. Hayakawa K, Okazaki R, Morioka K, Nakamura K, Tanaka S, Ogata T. Lipopolysaccharide preconditioning facilitates M2 activation of resident microglia after spinal cord injury. J Neurosci Res. 2014;92(12):1647-58.
55. Gordon S. Alternative activation of macrophages. Nat Rev Immunol. 2003;3(1):23-35.
56. Mantovani A, Sica A, Sozzani S, Allavena P, Vecchi A, Locati M. The chemokine system in diverse forms of macrophage activation and polarization. Trends Immunol. 2004;25(12):677-86.
57. Bogie JF, Timmermans S, Huynh-Thu VA, Irrthum A, Smeets HJ, Gustafsson JA, et al. Myelin-derived lipids modulate macrophage activity by liver X receptor activation. PLoS One. 2012;7(9):e44998.
58. Wang X, Cao K, Sun X, Chen Y, Duan Z, Sun L, et al. Macrophages in spinal cord injury: phenotypic and functional change from exposure to myelin debris. Glia. 2015;63(4):635-51.
59. Boven LA, Van Meurs M, Van Zwam M, Wierenga-Wolf A, Hintzen RQ, Boot RG, et al. Myelin-laden macrophages are anti-inflammatory, consistent with foam cells in multiple sclerosis. Brain. 2006;129(Pt 2):517-26.
60. Paludan SR, Lovmand J, Ellermann-Eriksen S, Mogensen SC. Effect of IL-4 and IL-13 on IFN-gamma-induced production of nitric oxide in mouse macrophages infected with herpes simplex virus type 2. FEBS Lett. 1997;414(1):61-4.
61. Szczepanik AM, Funes S, Petko W, Ringheim GE. IL-4, IL-10 and IL-13 modulate A beta(1--42)-induced cytokine and chemokine production in primary murine microglia and a human monocyte cell line. J Neuroimmunol. 2001;113(1):49-62.

62. Cash E, Minty A, Ferrara P, Caput D, Fradelizi D, Rott O. Macrophage-inactivating IL-13 suppresses experimental autoimmune encephalomyelitis in rats. J Immunol. 1994;153(9):4258-67.
63. Sicotte M, Tsatas O, Jeong SY, Cai CQ, He Z, David S. Immunization with myelin or recombinant Nogo-66/MAG in alum promotes axon regeneration and sprouting after corticospinal tract lesions in the spinal cord. Mol Cell Neurosci. 2003;23(2):251-63.

Supplemental information

Table S1: Basso mouse scale (29)

Score	
0	No ankle movement
1	Slight ankle movement
2	Extensive ankle movement
3	Plantar placing of the paw with or without weight support OR Occasional, frequent or consistent dorsal stepping but no plantar stepping
4	Occasional plantar stepping
5	Frequent or consistent plantar stepping, no coordination OR Frequent or consistent plantar stepping, some coordination, paws rotated at initial contact and lift off
6	Frequent or consistent plantar stepping, some coordination, paws parallel at initial contact OR Frequent or consistent plantar stepping, mostly coordinated, paws rotated at initial contact and lift off
7	Frequent or consistent plantar stepping, mostly coordinated, paws parallel at initial contact and rotated at lift off OR Frequent or consistent plantar stepping, mostly coordinated, paws parallel at initial contact and lift off, and severe trunk instability
8	Frequent or consistent plantar stepping, mostly coordinated, paws parallel at initial contact and lift off, and mild trunk instability OR Frequent or consistent plantar stepping, mostly coordinated, paws parallel at initial contact and lift off, and normal trunk stability and tail down or up & down
9	Frequent or consistent plantar stepping, mostly coordinated, paws parallel at initial contact and lift off, and normal trunk stability and tail always up.

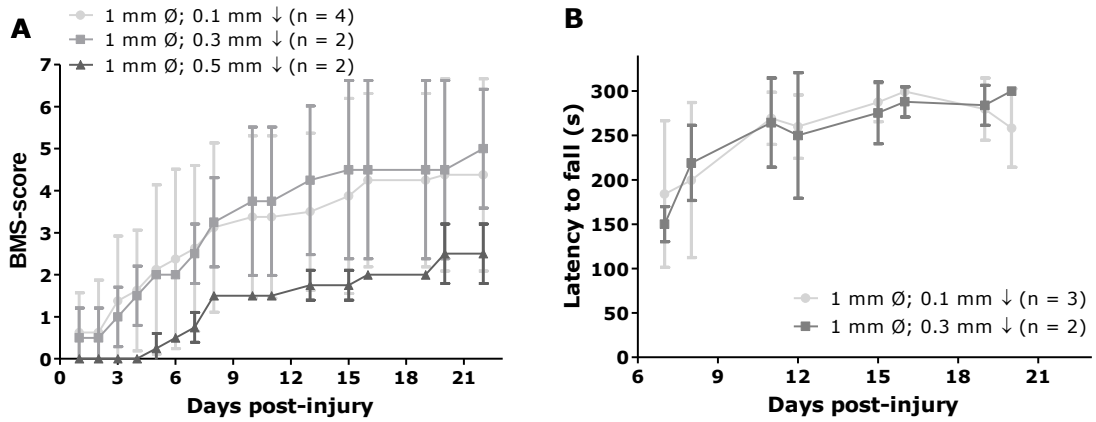

Figure S1: An unruptured dura after mild contusion SCI results in high mortality in contusions with 1 mm tip diameter. An impact diameter of 1 mm was tested with an impact depth of 0.1 mm, 0.3 mm or 0.5 mm. Functional recovery was analyzed via BMS scoring and rotarod performance analysis. High mortality was observed due to an unruptured dura, leading to increased pressure on the spinal cord and the brain. The animals of the 1 mm; 0.5 mm group are too severely injured and the error bars of the BMS score in the 0.1 and 0.3 mm groups are very large. The unruptured dura might have worsened the injury of the small impact depth group. This way, there is no clear difference seen in recovery between the 0.1 mm and 0.3 mm injury depths (A). Almost 50% of the surviving animals are excluded from rotarod performance analysis since they only use their forelimbs to stay on the rod. There is no difference in rotarod performance between the remaining animals (B). Data represent mean ± SD. BMS: Basso mouse scale. SCI: spinal cord injury.

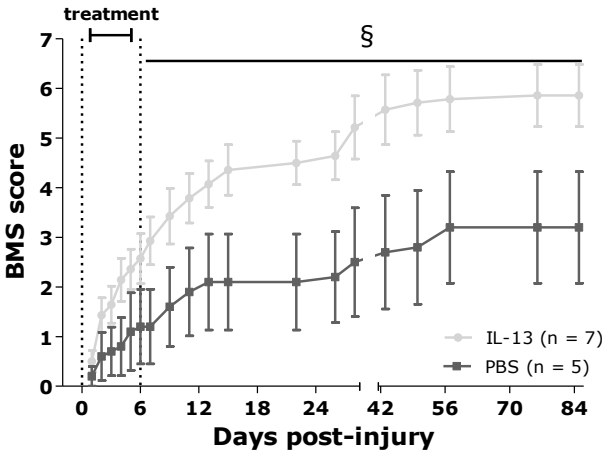

Figure S2: IL-13 improves functional recovery after hemisection SCI. Mice received a hemisection SCI at level T8-T10. Furthermore, they were treated with IL-13 or PBS for 7 sequential days starting at the day of surgery. Two-way ANOVA shows a significant difference between the two treatments groups from day 7 on (§) . The average BMS score on day 7 was 1.2 in the PBS-treated group, compared to 2.9 in the IL-13-treated group. These scores increase to 3.2 in the PBS group and 5.8 in the IL-13 group on day 85. Data represent mean ± SEM. § $p < 0.05$. BMS: Basso mouse scale. IL-13: Interleukin-13. PBS: Phosphate buffered saline.

Auteursrechtelijke overeenkomst

Ik/wij verlenen het wereldwijde auteursrecht voor de ingediende eindverhandeling:
Establishing a moderate contusion spinal cord injury mouse model and testing the therapeutic potential of interleukin-13

Richting: **master in de biomedische wetenschappen-klinische moleculaire wetenschappen**
Jaar: **2015**

in alle mogelijke mediaformaten, - bestaande en in de toekomst te ontwikkelen - , aan de Universiteit Hasselt.

Niet tegenstaand deze toekenning van het auteursrecht aan de Universiteit Hasselt behoud ik als auteur het recht om de eindverhandeling, - in zijn geheel of gedeeltelijk -, vrij te reproduceren, (her)publiceren of distribueren zonder de toelating te moeten verkrijgen van de Universiteit Hasselt.

Ik bevestig dat de eindverhandeling mijn origineel werk is, en dat ik het recht heb om de rechten te verlenen die in deze overeenkomst worden beschreven. Ik verklaar tevens dat de eindverhandeling, naar mijn weten, het auteursrecht van anderen niet overtreedt.

Ik verklaar tevens dat ik voor het materiaal in de eindverhandeling dat beschermd wordt door het auteursrecht, de nodige toelatingen heb verkregen zodat ik deze ook aan de Universiteit Hasselt kan overdragen en dat dit duidelijk in de tekst en inhoud van de eindverhandeling werd genotificeerd.

Universiteit Hasselt zal mij als auteur(s) van de eindverhandeling identificeren en zal geen wijzigingen aanbrengen aan de eindverhandeling, uitgezonderd deze toegelaten door deze overeenkomst.

Voor akkoord,

Donders, Ellen

Datum: **9/06/2015**